energy&fuels

pubs.acs.org/EF

Article

Applicability and Limitation of Aromatic Maturity Parameters in High-Maturity Oil from Ultradeep Reservoirs

Donglin Zhang, Meijun Li,* Rongzhen Qiao, and Hong Xiao

Cite This: *Energy Fuels* 2024, 38, 18413−18430

Read Online

ACCESS | Metrics & More | Article Recommendations

ABSTRACT: A substantial reserve of highly mature light oil has been discovered in the Ordovician reservoir of the Shunbei oilfield, Tarim Basin, Northwest China. This study aims to provide an objective assessment of oil maturity in the Shunbei oilfield and establish a reliable maturity evaluation index for oil in the high thermal evolution stage. Eighteen crude oil samples from the no. 4 fault zone (F4) of the Shunbei oilfield were systematically analyzed. Aromatic hydrocarbon, light hydrocarbon components, and diamondoid compositions were analyzed by gas chromatography−mass spectrometry. The depositional environment and the organic matter input of their related source rocks were determined by the corresponding geochemical indicators. The results indicate that the F4 oils have been derived from the same source kitchen and belong to the same oil population. The oil maturity in the study area was evaluated by the maturity parameters relative to aromatics, light hydrocarbons, and diamondoids. The analysis indicates that the results of aromatic parameters for identifying oil maturity contradict those of light hydrocarbon and diamondoid parameters. The equivalent vitrinite reflectance of the oil samples ranges from 1.43% to 1.54%. It is concluded that light hydrocarbon and diamondoid parameters can reliably be used to evaluate the maturity of oil in the high thermal evolution stage. However, most of the aromatic maturity parameters exhibit significant limitations during the high-temperature evolution stage. The maturity parameters of phenanthrene and dibenzothiophene were "reversed" in the high thermal evolution stage due to demethylation and thermal alteration, respectively. Additionally, most naphthalene maturity parameters are affected by thermally induced condensation, rendering them unsuitable for maturity evaluation of the high-temperature evolution stage. Notably, pentamethylnaphthalene ratio [PMNr, PMNr = 1, 2, 4, 6, 7-/(1, 2, 4, 6, 7 + 1, 2, 3, 5, 6)-pentamethylnaphthalene] exhibits a strong positive correlation with gas−oil ratio, *n*-heptane/methylcyclohexane (nC_7/MCH) ratio, and (3 + 4)-methyldiamantane concentrations, indicating their reliability as maturity indicators for highly to overmature oils and source rocks.

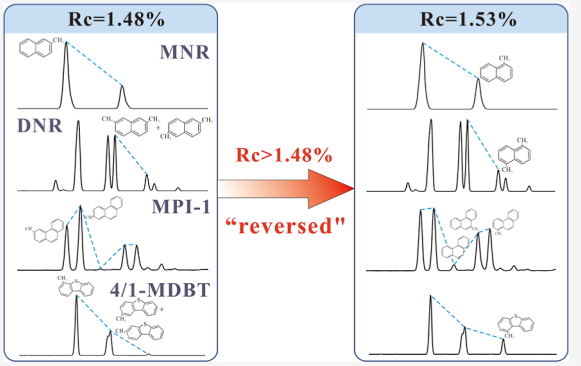

1. INTRODUCTION

Maturity serves as a crucial parameter in characterizing the availability of source rocks and elucidating petroleum properties.[1] Throughout various stages of thermal evolution, oil exhibits distinct physical and geochemical characteristics. Accurate identification of maturity levels not only enables the prediction of petroleum conversion degrees and the stage of oil formation but also provides invaluable guidance for petroleum exploration efforts.[2]

The concept of vitrinite reflectance (Ro) originally emerged in coal petrology as a means to assess coal rank.[3−5] It quantifies the ratio of reflected light to vertical incident light intensity on a polished surface of homogeneous vitrinite or matrix vitrinite in coal under oil immersion conditions. Teichmuller (1950) later extended the application of vitrinite reflectance (Ro) to assess the maturity of dispersed organic matter in sedimentary rocks. Over time, Ro has evolved into the most widely used and reliable indicator of maturity, offering objective insights into the maturation levels of organic matter in most source rocks since the late Paleozoic era.[6,7]

The stability and configuration evolution of biomarkers and hydrocarbons within oil undergo notable transformations during thermal evolution. To effectively assess crude oil maturity, researchers have developed the concept of equivalent vitrinite reflectance (% Rc), which considers the variation patterns of various parameters in thermal evolution and their coupling relationship with vitrinite reflectance (Ro).[8−10] This approach provides a new "window" for evaluating crude oil's

Received: May 8, 2024
Revised: August 30, 2024
Accepted: September 5, 2024
Published: September 18, 2024

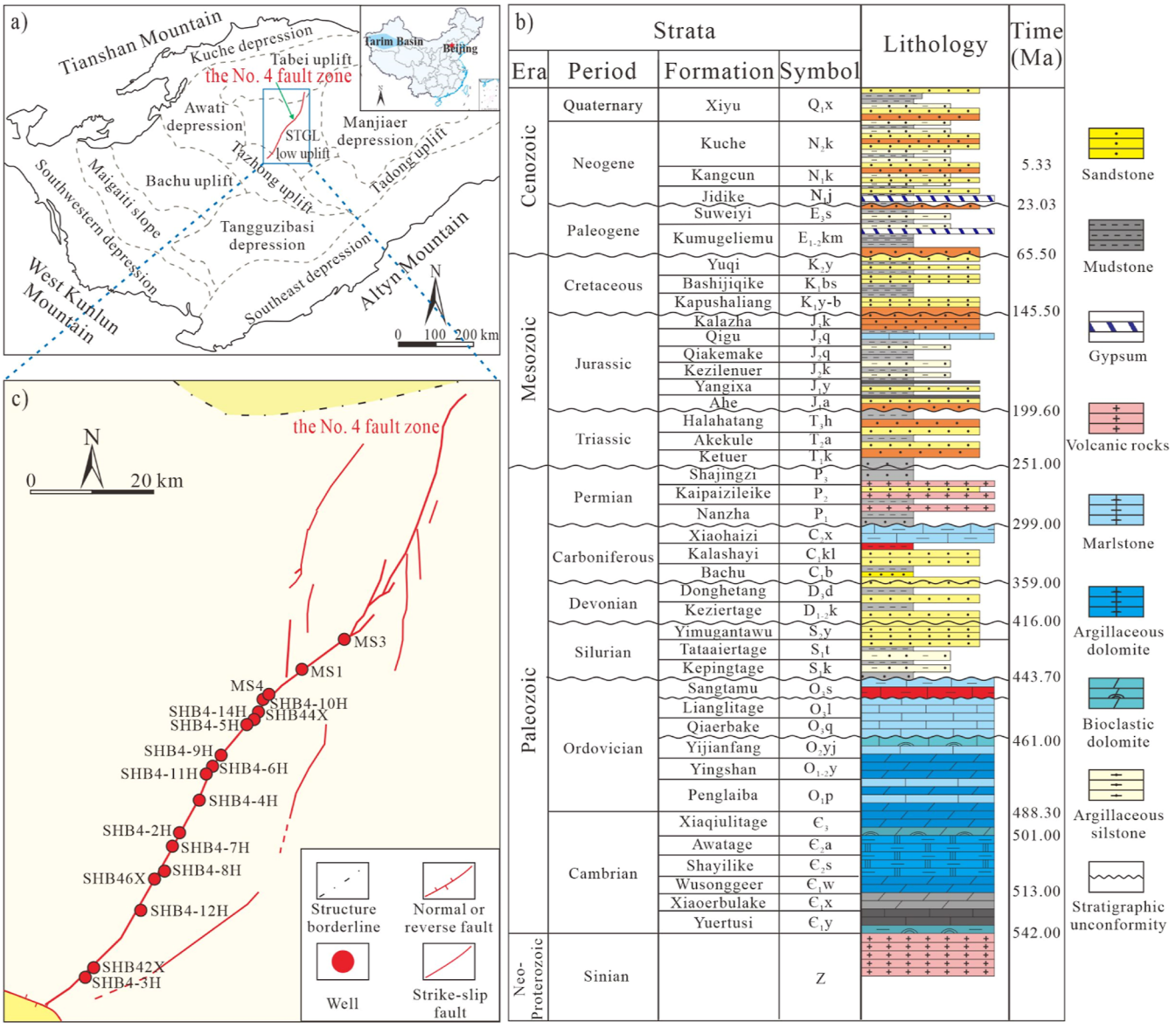

Figure 1. (a) Map showing the location of the Tarim Basin; (b) generalized stratigraphic column in the STGL Low Uplift (reproduced with permission from ref 47. Copyright 2024 Elsevier); (c) map showing locations of the sampled wells in no. 4 fault zone (F4) of the Shunbei oilfield (reproduced with permission from ref 47. Copyright 2024 Elsevier).

maturity levels, enhancing our understanding of its thermal history and geochemical characteristics.

During thermal evolution, parameters related to saturated hydrocarbons undergo changes due to thermal cracking and stability, typically offering insights into the maturation of crude oil within the low to mature stages.[11−13] However, in highly mature samples, aromatic biomarkers exhibit abundant concentrations.[14−16] Additionally, the thermal stability disparity between α- and β-substituent isomers is significant during the high thermal evolution stage,[9,17] making them valuable for evaluating crude oil maturity in advanced evolutionary stages.[18,19]

Light hydrocarbons, constituting a significant portion of oil, often exceed 90% of the total components in light oils, including volatile oils and condensate.[20] Consequently, the geochemical information embedded within light hydrocarbons holds particular significance for understanding light oils.[21,22] Maturity parameters associated with light hydrocarbons have been extensively employed in basins worldwide. Thompson (1979) observed a strong correlation between *n*-heptane/methylcyclohexane (nC_7/MCH) and maturity.[23] Subsequently, heptane value (H) and isoheptane value (I) were proposed in 1983 as indicators for evaluating petroleum maturity stages. Mango (1987) established a significant correlation between 2, 4-/2, 3-dimethylpentane (2, 4-/2, 3-DMP) and formation temperature, suggesting its utility in indicating maturity levels.[24] Hou et al. (1989) identified isobutene/*n*-butane (iC_4/nC_4) and isopentane/*n*-pentane (iC_5/nC_5) as effective maturity indicators during the early thermal evolution of organic matter, although these parameters become ineffective when Ro exceeds 0.8%.[25] Additionally, Chen et al. (2009) discovered that 2, 2-dimethylbutane/*n*-hexane (2, 2-DMB/nC_6) and (2- + 3-methylcyclohexane)/*n*-heptane [(2-MCH + 3-MCH)/nC_7] exhibit corresponding changes with increasing crack temperature during the analysis of light hydrocarbon components in Tarim oils, thereby serving as effective maturity indicators.[26]

https://doi.org/10.1021/acs.energyfuels.4c02159
Energy Fuels 2024, 38, 18413−18430

Furthermore, diamondoids represent a class of cage-type hydrocarbon compounds that are characterized by exceptional thermal stability. Formed from organic parent material through carbon ion mediation in acidic conditions, diamondoids are commonly observed in highly mature oil reservoirs.[27] Owing to their unique molecular structure and remarkable thermal stability, diamondoids hold significant potential for evaluating oils at highly mature stages.[28−30] Chen et al. (1996) initially proposed the methyladamantane index [MAI, MAI = 100 × 1-MA/(2-MA + 1-MA), MA: methyladamantane] and the methyldiamantane index [MDI, MDI = 100 × 4-MD/(4-MD + 1-MD + 3-MD), MD: methyldiamantane] for assessing the maturity of oil and condensate in petroleum basins in China.[28] Subsequently, numerous studies have explored the assessment of crude oil maturity based on diamondoid parameters, including the ethyladamantane index [EAI, EAI = 1-EA/(2-EA + 1-EA), EA: ethyladamantane], dimethyladamantane index 1 [DMAI-1, DMAI-1 = 1, 3-DMA/(1, 3-DMA + 1, 2-DMA), DMA: dimethyladamantane], dimethyldiamantane index 2 [DMDI-2, DMDI-2 = 3, 4-DMD/(4, 9-DMD + 3, 4-DMD), DMD: dimethyldiamantane], A/D (adamantane/diamantane), MA/MD (methyladamantane/methyldiamantane), and others.[31−33]

As the global petroleum industry advances and energy demands escalate, petroleum exploration has extended to ultradeep basins.[34] However, most of the ultradeep petroleum is in high thermal evolution, and the conventional maturity evaluation parameters are limited to different degrees.[2,15,35] For instance, Radke and Welte (1983) observed an "inversion" of the MPI-1 [MPI-1 = 1.5 × (2-MP + 3-MP)/(P + 1-MP + 9-MP), MP: methylphenanthrene] value at Ro > 1.35%.[8] Wang et al. (2022) highlighted a similar phenomenon with a series of methylnaphthalene parameters [including tetramethylnaphthalenes (TeMNs), trimethylnaphthalenes (TMNs), and dimethylnaphthalenes (DMNs)] exhibiting a "reverse" trend when Ro > 1.1% due to the transition from methylation and rearrangement to demethylation.[35] Consequently, the utilization of aromatic parameters for evaluating the maturity of ultradeep petroleum has been controversial.

Currently, the ultradeep buried (>7000 m) Ordovician reservoir within the Shunbei oilfield, situated in the Tarim Basin (Northwest China), has yielded substantial volumes of volatile oil and condensate. Previous studies have extensively examined petroleum maturity evaluation in this region. Wang et al. (2021) utilized aromatic maturity parameters [Rc1 = 0.6 × MPI-1 + 0.4, Rc2 = 0.036 × (4-/1-MDBT) + 0.56, MDBT: methyl dibenzothiophene] and determined the Rc of F5 and F1 to range from 0.77% to 0.86% and 0.90% to 1.53%, respectively.[15] Chen et al. (2021) employed diamondoid parameters (Rc3 = 0.0243 × MDI + 0.4389) and calculated the Rc of F1 oil to be between 1.26% and 1.45%.[36] Additionally, Bian et al. (2023) utilized aromatic maturity parameters [Rc4 = 0.49 + 0.09 × DNR, DNR= (2, 7- + 2, 6-)/1, 5-DMN, DMN: dimethylnaphthalene] and derived the Rc of F5 ranging from 1.03% to 1.60%.[37] Overall, the maturity levels of F5 and F1 appear to be low, with various maturity evaluation parameters demonstrating effective application. However, for the oils in the no. 4 fault zone (F4 oils) with higher maturity, the suitability of different maturity evaluation parameters requires further discussion.

This study focuses on the analysis of 18 oil samples collected from F4 of the Shunbei oilfield. Analyses using gas chromatography (GC) were conducted on whole-oil samples, while gas chromatography−mass spectrometry (GC−MS) analyses were performed to examine saturated and aromatic hydrocarbons. Additionally, diamondoid analysis was carried out to complement the assessment of petroleum maturity. The study aims to compare and analyze the applicability of aromatic, light hydrocarbon, and diamondoid parameters in evaluating maturity levels comprehensively. By delineating the effective application range of various maturity parameters, this research aims to provide reliable guidance for selecting parameters for evaluating the maturity of oil in high-temperature evolution stages.

2. GEOLOGICAL BACKGROUND

Tarim Basin, located in Northwest China with an area of about 5.6×10^5 km^2, is the largest petroleum basin in China (Figure 1).[38] The Tarim Basin can be divided into 12 tectonic units, which are Southeast Depression, Southwestern Depression, Tangguzibasi Depression, Maigaiti Slope, Bachu Uplift, Tazhong Uplift, Tadong Uplift, Manjiaer Depression, Shuntuoguole Low Uplift (STGL Low Uplift), Awati Depression, Tabei Uplift, and Kuche Depression form south to north (Figure 1).[39] Undergoing multistage tectonic evolution, the Tarim Basin is characterized as a multicycle superimposed petroleum basin comprising meso-Cenozoic foreland basins and Paleozoic craton basins with complex hydrocarbon accumulation and distribution.[40,41] The strata mainly include the Sinian−Devonian marine sequence, the Carboniferous−Permian marine−terrestrial transitional sequence, and the Triassic−Quaternary terrestrial sequence (Figure 1).[33,42]

The Shunbei oilfield is mainly located in STGL, a low uplift in the abdomen of the Tarim Basin (Figure 1). The STGL Low Uplift is adjacent to the Katake Uplift in the south and Shaya Uplift in the north.[43] Several strike-slip faults developed within it. Among them, the western fault zone is mostly NW-striking, while the eastern fault zone is mostly NE-striking.[44] As an ultradeep petroleum area with huge exploration potential, major breakthroughs have been made in the petroleum exploration of Ordovician marine carbonate rocks in the recent years.[41] The carbonate rocks of Yijianfang Formation (O_2yj) and Yingshan Formation ($O_{1-2}y$) form a very good reservoir cap combination with the superthick mudstone cap of Sangtamu Formation (O_3s), which is the main target reservoir for petroleum exploration evaluation at present.[37] The proved oil depth in the Shunbei oilfield is more than 7200 m, and the reservoir types are mainly fractures, solution holes, and caves.[15]

3. SAMPLES AND METHODS

3.1. Samples. Eighteen Ordovician oil samples were collected in the wellhead, and the samples were evenly distributed in the north, middle, and south of F4. Samples collected from the wellhead are refrigerated in sealed vials to prevent the volatilization of light components. After the samples were transferred to the laboratory, the GC analyses of whole oil and GC−MS analyses for saturated and aromatic hydrocarbons, light hydrocarbons, and diamondoid compounds were carried out.

3.2. Methods. *3.2.1. GC Analysis.* The analysis of whole oil was conducted on an Agilent 6890GC instrument fitted with an HP-PONA quartz capillary column (50 × 0.2 mm × 0.5 μm). Initially, the oven's temperature was set to 35 °C for 10 min, followed by a ramp up to 60 °C at 0.5 °C/min, and then increased to 200 °C at 2 °C/min, ultimately held at 300 °C for 10 min.

3.2.2. GC−MS Analysis. The saturated and aromatic fractions of Shunbei oil were analyzed using GC−MS. The oil was separated by silica gel and alumina column chromatography with petroleum ether, a mixture of petroleum ether and dichloromethane (2:1, v−v), and a

https://doi.org/10.1021/acs.energyfuels.4c02159
Energy Fuels 2024, 38, 18413−18430

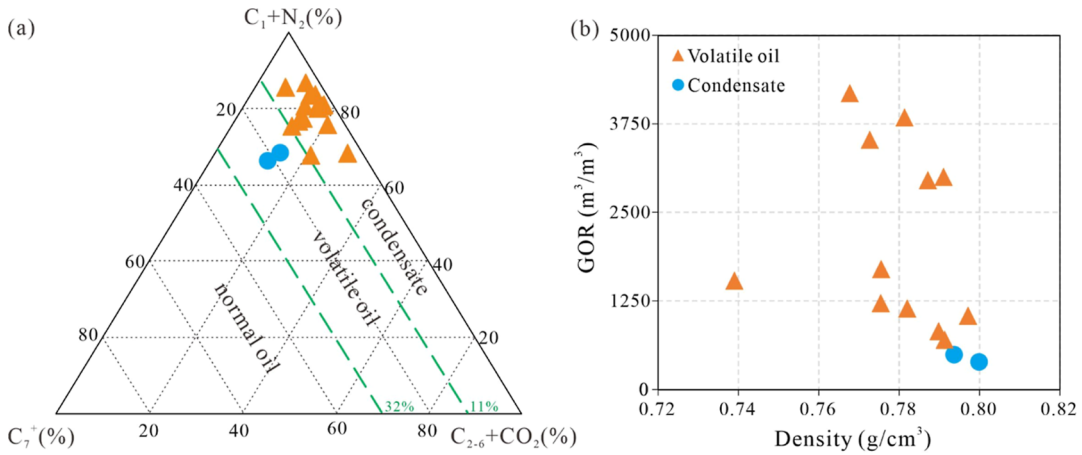

C_1: CH_4; N_2: nitrogen; C_{2-6}: the sum of hydrocarbon with a carbon number between 2 and 6; CO_2: carbon dioxide; C_7^+: the sum of hydrocarbon with a carbon number great than or equal to 7.

Figure 2. Petroleum bulk properties of the no. 4 fault zone (F4) in the Shunbei oilfield: (a) reservoir fluid ternary diagram; (b) relationship between gas−oil ratios (GORs) and the density of oils.

Table 1. Physical Properties of the Oil Samples in This Study[a]

well	depth (m)	strata	density (g/cm^3)	viscosity (mm^2/s)	sulfur (%)	wax (%)	GOR (m^3/m^3)	type
MS3	7550.00−8083.00	O_2yj−$O_{1-2}y$	0.80	1.39	0.0870	10.70	393	volatile oil
MS1	7535.00−8050.00	O_2yj−$O_{1-2}y$	0.79	1.37	0.1180	11.85	496	
MS4	7573.00−8202.00	O_2yj−$O_{1-2}y$	0.79	0.93	0.2330	7.86	702	condensate
SHB4-10H	7487.00−8126.57	O_2yj−$O_{1-2}y$	0.79	2.09	0.0895	2.20	825	
SHB44X	7499.00−8261.69	O_2yj−$O_{1-2}y$	0.80	2.03	0.0936	5.40	1044	
SHB4-14H	7551.50−7932.80	O_2yj−$O_{1-2}y$					1449	
SHB4-5H	7729.00−8850.34	O_2yj−$O_{1-2}y$	0.78	1.80	0.0764		1147	
SHB4-9H	7600.00−8110.17	O_2yj−$O_{1-2}y$	0.74	0.89	0.0531	4.40	1539	
SHB4-6H	7571.75−8356.02	O_2yj−$O_{1-2}y$	0.78	1.76	0.0576	2.40	1220	
SHB4-11H	7794.98−9057.45	O_2yj−$O_{1-2}y$		2.43	0.0079	1.00	2441	
SHB4-4H	7607.00−8483.70	O_2yj−$O_{1-2}y$		5.01	0.0704	4.60	3500	
SHB4-2H	7552.00−8587.04	O_2yj−$O_{1-2}y$		1.20	0.0693	3.20	3387	
SHB4-7H	7877.00−8145.10	O_2yj−$O_{1-2}y$	0.77	1.24	0.0962		4182	
SHB4-8H	7950.00−8378.00	O_2yj−$O_{1-2}y$	0.79	1.77	0.0566	4.00	2955	
SHB46X	8600.00−8670.00	O_2yj−$O_{1-2}y$	0.78	1.84	0.0727	4.70	1702	
SHB4−12H	7601.50−8630.24	O_2yj−$O_{1-2}y$	0.78	1.77	0.2190	3.20	3841	
SHB42X	7392.00	O_2yj−$O_{1-2}y$	0.77	1.43	0.1760	8.66	3526	
SHB4-3H	7386.00−8179.64	O_2yj−$O_{1-2}y$	0.79	1.95	0.1660	5.00	3002	

[a]GOR = gas-to-oil ratio, "/" = no data.

mixture of dichloromethane and methyl alcohol (93:7, v−v). The saturated hydrocarbon, aromatic hydrocarbon, and nonhydrocarbon components are obtained sequentially. Analysis of saturated and aromatic hydrocarbons utilized Agilent 6890GC/5975iMSD and 7890GC/5977MS instruments, respectively, coupled with an HP-5MS (60 m × 0.25 mm × 0.25 μm) fused silica capillary column. Saturated hydrocarbon GC−MS analysis conditions: the GC oven temperature was set to 50 °C for 1 min, subsequently increasing to 100 °C at 20 °C/min, followed by a ramp to 310 °C at 3 °C/min, finally held at 310 °C for 10 min. Aromatic hydrocarbon GC−MS analysis conditions: the GC oven temperature was set to 80 °C for 1 min, then gradually raised to 310 °C at 3 °C/min, and maintained at 310 °C for 20 min.

Analysis for diamondoids utilized an Agilent 6890GC/5975MS instrument. Diamondoid GC−MS analysis conditions: initially set at 50 °C for 1 min, then ramped up to 250 °C at 3 °C/min, and further increased to 310 °C with a heating rate of 20 °C/min before being held for 10 min. D16-adamantane was added to the Shunbei oil samples as an internal standard.

4. RESULTS

4.1. Bulk Properties. Based on the ternary diagram of reservoir fluid analysis, it was determined that the F4 reservoir primarily constitutes a condensate reservoir, with only two volatile oil reservoirs (e.g., MS1 and MS3) identified at the northernmost end of the fault zone (Figure 2). The physical properties of F4 oils are in alignment with those of the reservoir type (Figure 2). Volatile oil exhibits a high density (0.79−0.80 g/cm^3), elevated wax content (10.70−11.85%), and a relatively low GOR (393−496 m^3/m^3) (Table 1). Conversely, the condensate displays a lower wax content (1.00−8.66%) and density (0.74−0.80 g/cm^3), alongside a higher GOR (702−4182 m^3/m^3) (Table 1).

4.2. Normal Alkanes and Biomarkers. The GC analysis of whole oil revealed an intact *n*-alkane series (nC_6 to nC_{34}) within the F4 oil samples. Moreover, there was no notable presence of "hump" (unresolved complex mixture, UCM), suggesting little significant biodegradation effects on the samples in this area (Figure 3).[45] The *n*-alkane series exhibited a unimodal

https://doi.org/10.1021/acs.energyfuels.4c02159
Energy Fuels 2024, 38, 18413−18430

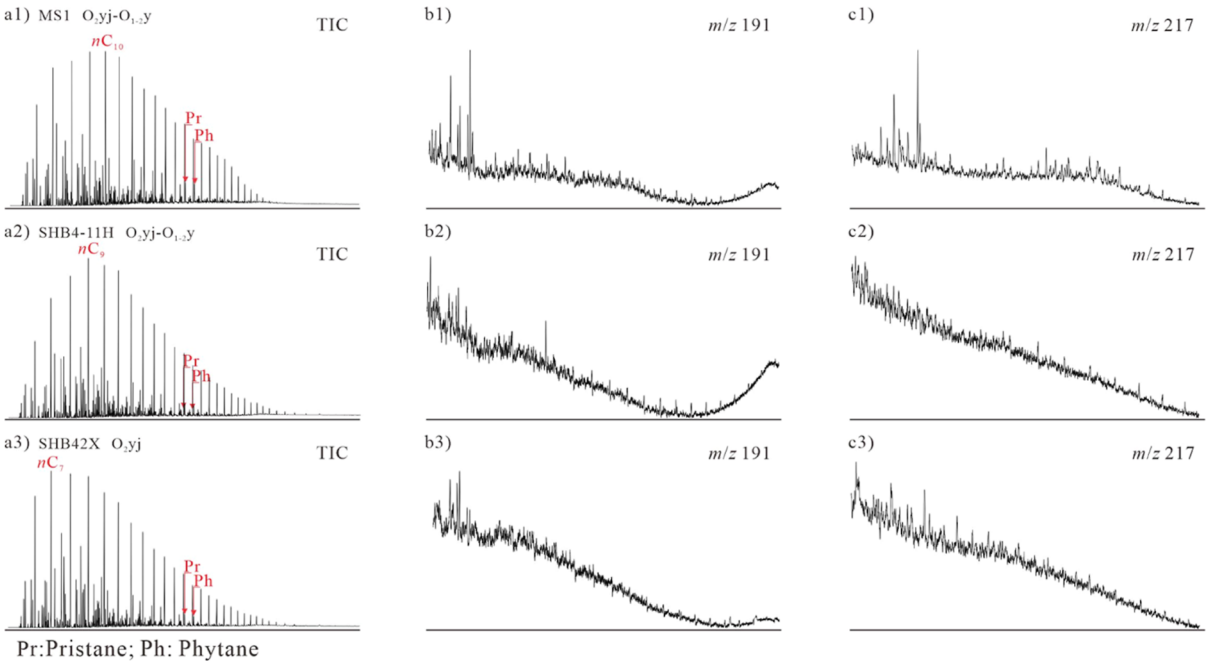

Figure 3. Mass chromatograms showing the distribution of alkanes (a1−a3), terpanes (b1−b3), and steranes (c1−c3).

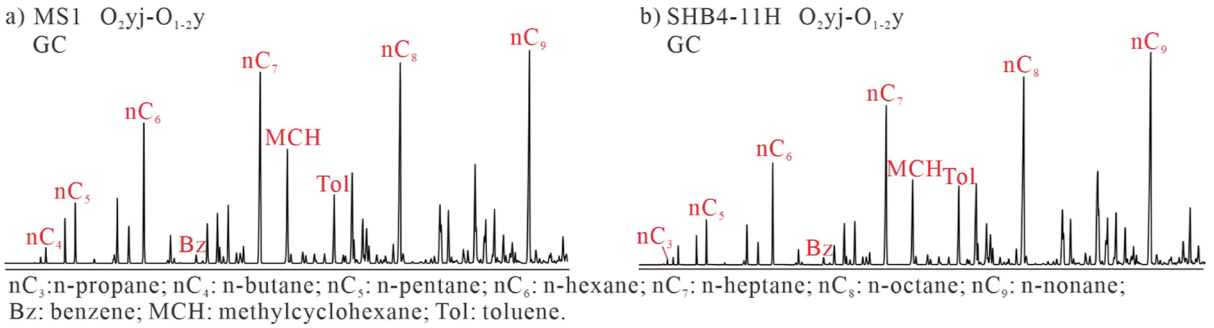

Figure 4. Gas chromatograms showing the distribution of C_3−C_9 light hydrocarbons.

distribution, predominantly comprising short-chain *n*-alkanes. The dominant peak carbon numbers ranged from C_7 to C_{10}, indicating the input of organic matter derived from marine algae.[46]

Furthermore, the mass spectrograms of *m*/*z* 191 and *m*/*z* 217 revealed that the concentrations of conventional steranes and terpenes in the saturated hydrocarbons of F4 oils were significantly lower than the detected values. This indicates that the F4 oils are at a high level of thermal maturity or have suffered secondary alteration processes such as thermal alteration (Figure 3).[47]

4.3. Light Hydrocarbons and Diamondoids. Despite their low content of saturated hydrocarbons, F4 oils contain abundant light hydrocarbons and diamondoid compounds. Light hydrocarbon compounds of the C_3−C_9 range can be detected in F4 oils (Figure 4). Among these, C_7 emerged as the most abundant light hydrocarbon compound, constituting 17.32% to 27.76% of the total light hydrocarbon content. The composition of C_7 light hydrocarbons primarily comprised alkanes, cycloalkanes, and aromatics, with normalized percentages ranging from 54.20% to 60.08%, 16.85% to 29.20%, and 12.29% to 27.87%, respectively (Table 2). Notably, Figure 5 illustrates significant variations in the content of cycloalkanes and aromatics between the oils from the southern and northern regions of F4, suggesting potential differences in maturity levels.

Additionally, mass chromatograms (Figure 6) revealed the presence of adamantanes and diamantanes at *m*/*z* 136, 135, 149, 163, 188, 187, and 201. The total diamondoid concentrations ranged from 806.83 to 5479.55 μg/g oil, with adamantane concentrations ranging from 703.25 to 4963.67 μg/g oil and diamantane concentrations ranging from 80.15 to 462.25 μg/g oil (Table 3). The elevated concentration of diamondoids in oil suggests a potentially higher stage of thermal evolution for the oils.

5. DISCUSSION

5.1. Oil Family Classification. F4 oils had a range of pristane/phytane (Pr/Ph) ratios from 0.91 to 1.30, with an average ratio of 1.14, indicating characteristics typical of a reduced depositional environment (Table 2).[10] Analysis of the Pr/nC_{17} versus Ph/nC_{18} cross-plot suggests that the organic matter source for the F4 oils is predominantly type II organic matter (Figure 7). The samples exhibit a linear distribution on the chart, suggesting similar depositional environments.

Previous research has established that methylcyclohexane (MCH) primarily originates from lignin in higher plants, dimethylcyclopentane (DMCP) is derived from lipid com-

https://doi.org/10.1021/acs.energyfuels.4c02159
Energy Fuels 2024, 38, 18413−18430

Table 2. Biomarkers and Hydrocarbon Components for Identification of the Organic Input and Depositional Environment of the Shunbei Oil[a]

well	Pr/Ph	Pr/nC_{17}	Ph/nC_{18}	alkanes	cycloalkanes	aromatics	4, 8-DMD	4, 9-DMD	3, 4-DMD
					C_7, %			%	
MS3	1.07	0.29	0.32	59.73	27.85	12.42	0.34	0.23	0.44
MS1	0.91	0.29	0.22	58.51	29.20	12.29	0.34	0.23	0.43
MS4	1.04	0.27	0.31	60.08	26.52	13.40	0.34	0.23	0.43
SHB4-10H	1.06	0.28	0.30	57.94	27.09	14.97	0.34	0.23	0.42
SHB44X	1.08	0.26	0.29	57.72	25.57	16.71	0.33	0.23	0.44
SHB4-14H	1.10	0.26	0.27	59.64	23.99	16.37	0.31	0.23	0.46
SHB4-5H	1.17	0.27	0.26	57.23	24.89	17.88	0.33	0.23	0.44
SHB4-9H	1.12	0.25	0.26	58.74	24.16	17.10	0.33	0.24	0.43
SHB4-6H	1.16	0.24	0.24	57.84	23.69	18.47	0.33	0.23	0.43
SHB4-11H	1.16	0.21	0.21	56.98	25.22	17.81	0.31	0.22	0.47
SHB4-4H	1.14	0.17	0.17	57.69	19.43	22.88	0.33	0.23	0.44
SHB4-2H	1.12	0.15	0.16	55.28	16.85	27.87	0.35	0.24	0.42
SHB4-7H	1.27	0.15	0.15	55.44	17.94	26.62	0.36	0.24	0.40
SHB4-8H	1.24	0.18	0.16	56.77	20.03	23.20	0.36	0.24	0.40
SHB46X	1.30	0.10	0.10	59.40	20.69	19.92	0.34	0.23	0.42
SHB4-12H	1.28	0.13	0.13	54.20	18.10	27.70	0.35	0.24	0.41
SHB42X	1.17	0.24	0.25	58.21	19.49	22.30	0.37	0.24	0.39
SHB4-3H	1.11	0.25	0.26	56.82	19.58	23.59	0.37	0.24	0.39

[a]DMD: dimethyldiamantane.

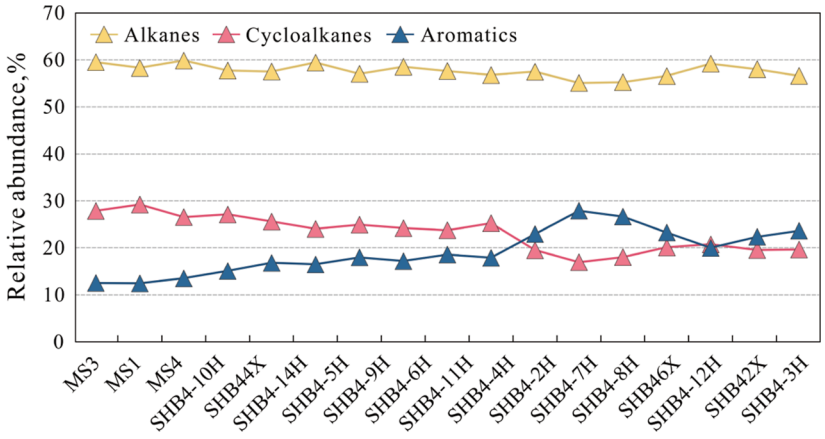

Figure 5. Relative abundance of alkanes, cycloalkanes, and aromatics among C_7 light hydrocarbons.

pounds in aquatic organisms, and nC_7 is predominantly contributed by algae and bacteria.[48] Consequently, the nC_7-ΣDMCP-MCH triangle diagram is commonly employed to differentiate the organic matter source of oil and source rock.[48] As shown in Figure 8, F4 oils exhibit a pronounced predominance of nC_7 and share similar distribution characteristics, suggesting that the sapropel type primarily constitutes the organic matter source in the Shunbei oilfield.

Furthermore, studies indicate that diamondoid parameters predominantly represent products synthesized by source rocks during high thermal evolution stages, serving to distinguish organic input and depositional environments.[31] As demonstrated in Figure 8, oils from the study area exhibit good aggregation and a consistent distribution range, indicating a common organic matter source. According to the regional template outlined by Schulz et al. (2001), the organic input of F4 samples is identified as marine type II sapropelic organic matter.[31]

Through the study of sulfur isotope values and the characteristics of aryl isoprene compounds, researchers concluded that the Tarim oil originates from the Cambrian Yuertusi Formation source rocks.[49,50] Based on the above analysis, we argue that the F4 oils in the Shunbei oilfield belong to the same oil population and were derived from a common source bed, which is also a prerequisite of our discussion of maturity parameters.

5.2. Maturity Assessment of Oil. *5.2.1. Maturity Assessment Based on Light Hydrocarbons.* As the thermal maturity increases, the alkylation degree of oil increases gradually. Based on this, Thompson (1983) proposed that using the heptane value (H) and the isoheptane value (I) could serve as indicators to identify the maturity of oil.[51] Subsequently, Walters et al. (2003) further improved this chart and gave the distribution interval corresponding to the % Rc.[52] The distribution ranges of H and I values of F4 oils are 37.26−48.12% and 2.57−3.64%, respectively, with an average of 42.23% and 3.02% (Table 3). The oil samples are at a high maturity stage with a Rc range of 1.3−1.6% (Figure 9).

Thompson (1987) analyzed in detail the distribution of paraffin index (F, F = nC_7/MCH) and H value in 76 oil samples

https://doi.org/10.1021/acs.energyfuels.4c02159
Energy Fuels 2024, 38, 18413−18430

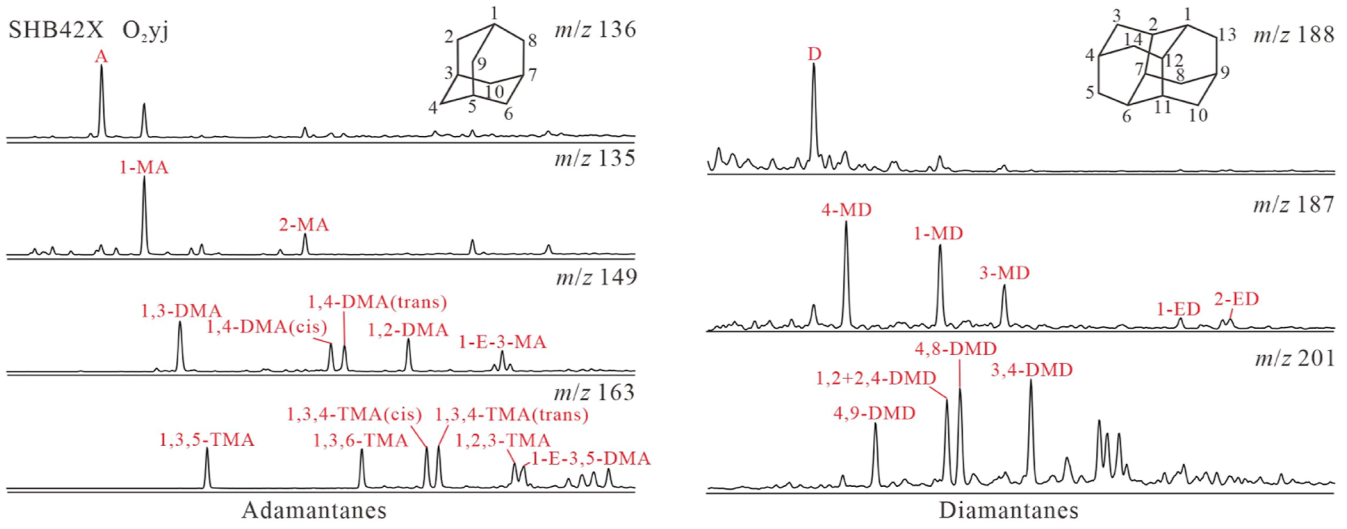

A: adamantane; 1-MA: 1-methyladamantane; 2-MA: 2-methyladamantane; 1, 3-DMA: 1, 3-Dimethyladamantane;1, 4-DMA: 1, 4-Dimethyladamantane; 1, 2-DMA: 1, 2-Dimethyladamantane;1-E-3-MA: 1-Ethyl-3-methyladamantane; 1, 3, 5-TMA: 1, 3, 5-Trimethyladamantane; 1, 3, 6-TMA: 1, 3, 6-Trimethyladamantane; 1, 3, 4-TMA: 1, 3, 4-Trimethyladamantane; 1, 2, 3-TMA: 1, 2, 3-Trimethyladamantane; 1-E-3, 5-DMA: 1-Ethyl-3, 5-dimethyladamantane; D: Diamantane; 4-MD: 4-Methyldiamantane; 1-MD: 1-Methyldiamantane; 3-MD: 3-Methyldiamantane; 1-ED: 1-Ethyldiamantane; 2-ED: 2-Ethyldiamantane; 4, 9-DMD: 4,9-Dimethyldiamantane; 1, 2-+2, 4-DMD:1, 2-+2, 4-Dimethyldiamantane; 4, 8-DMD: 4, 8-Dimethyldiamantane; 3, 4-DMD: 3, 4-Dimethyldiamantane.

Figure 6. Representative mass chromatograms showing the distributions of some diamondoid compounds.

from the north of the United States and found that the two showed an obvious positive correlation.[53] Therefore, the B−F (B = Tol/nC_7, Tol: toluene) chart proves to be a valuable tool for assessing oil maturity. Figure 9 shows that there are some differences in the maturity of oil samples in the Shunbei oilfield. Notably, the oil maturity in the southern region of F4 was markedly higher than that in the northern region, as depicted in Figure 9. Therefore, we divide the F4 oils into two parts (north and south) for the following discussion.

5.2.2. Maturity Assessment Based on Diamondoids. Due to their high thermal maturity, diamondoid compounds with high thermal stability were used for further maturity analysis.[32] F4 oils contain abundant diamondoid compounds, with total diamondoid concentrations all exceeding 800.00 μg/g of oil and reaching up to 5479.55 μg/g of oil. Previous studies have shown that diamondoid maturity parameters apply across a wide range of thermal evolutions. Secondary processes in the reservoir have little influence on diamondoid compounds, which strongly resist thermal cracking and biodegradation. Only under strong evaporative fractionation conditions can a significant amount of diamondoid compounds be lost.[54,55] The low degree of oil cracking in the Shunbei oilfield has no effect on the diamondoid compounds.[47] Analysis of adamantane concentration versus diamantane concentration and (1- + 2-) MA (MA: methyladamantanes) versus (3- + 4-) MD (MD: methyldiamantanes) concentration in F4 oils reveals robust linear relationships, with correlation coefficients of 0.9939 and 0.9910, respectively (Figure 10). This observation suggests that diamondoid parameters within the F4 oils remain unaffected by evaporative fractionation, affirming their reliability in oil maturity evaluation.

MAI and MDI, proposed by Chen et al. (1996), serve as reliable indices for evaluating highly mature oil.[28] In the study area, oil exhibited MAI and MDI values ranging from 73.19% to 79.13% and from 40.97% to 45.29%, respectively, averaging at 76.53% and 43.54% (Table 3). These values signify that the F4 oils have reached a high maturity stage and have an Rc range between 1.3% and 1.6% (Figure 11). This finding aligns with the results obtained from the parameters of light hydrocarbon maturity.

Subsequent integration of diamondoid maturity parameters, including EAI, DMAI-1, A/D, and MA/MD,[31−33] reveals discernible differences in oil maturity between the southern and northern regions of F4 (Figure 11). The Rc of F4 oils was calculated based on the formula Rc = 0.0243 MDI + 0.4389, and the results show that the Rc is 1.43%−1.50% in the north and 1.51%−1.54% in the south.[28] Consequently, it is inferred that diamondoid parameters, particularly MDI, accurately calculate the oil maturity.

5.2.3. Maturity Assessment Based on Aromatic Hydrocarbon Parameters. The biomarkers related to saturated hydrocarbons have poor stability and tend to crack at the high maturity stage.[11−13] Aromatic hydrocarbons exhibit higher thermal stability compared to saturated hydrocarbons, and their associated parameters can be utilized to evaluate the maturity level during high thermal evolution stages.[8,9,14]

In this paper, MPI-1; MPI-2 [MPI-2 = (2-MP)/(P + 9-MP + 1-MP) × 3]; 4-/1-MDBT (MDBT: methyl dibenzothiophene); 2, 4-/(1, 6- + 1, 4-)DMDBT (DMDBT: dimethyl dibenzothiophene); 4, 6-/(1, 6- + 1, 4-)DMDBT; TMNr [TMNr = 1, 3, 7-/(1, 2, 5- + 1, 3, 7-)TMN]; TeMNr [TeMNr = 1, 3, 6, 7-/(1, 2, 3, 5- + 1, 3, 6, 7- + 1, 2, 5, 6-)TeMN], and other aromatics maturity parameters were selected to assess the maturity of F4 oils. The results show that there are differences in oil maturity between the north and south subsection of the F4 (Figure 12 and Table 4). Interestingly, the aromatic hydrocarbon parameters showed the opposite result to the light hydrocarbon and diamondoid maturity parameters. The oil in the Shunbei oilfield belongs to the same oil population, so the organic input and depositional environment are not the reasons for this difference. Moreover, migration and mixed charging have no significant impact on aromatic maturity parameters in the Shunbei oilfield, according to previous studies, and the F5 with relatively low maturity has effectively applied the relevant parameters.[15,56] Oil properties (such as GOR, oil density, and viscosity) also indicate that the

https://doi.org/10.1021/acs.energyfuels.4c02159
Energy Fuels 2024, 38, 18413−18430

Table 3. Parameters Derived from Light Hydrocarbons and Diamondoids of the Shunbei Oil[a]

area	well	H	I	B	F	MAI	MDI	Rc	EAI	DMAI-1	A/D	MA/MD	(1- + 2-) MA	(3- + 4-) MD	total adamantanes	total diamantanes
															μg/g (oil)	
south subsection	MS3	37.26	2.61	0.33	1.89	74.66	42.27	1.47	55.16	61.59	1.55	4.81	157.97	21.73	703.25	80.15
	MS1	37.40	2.57	0.34	1.73	73.19	42.02	1.46	54.39	62.68	1.46	4.64	255.61	37.02	1143.09	133.62
	MS4	37.83	2.82	0.36	1.98	75.40	43.82	1.50	51.10	62.80	1.70	5.32	302.12	37.84	1346.27	139.31
	SHB4-10H	40.03	2.72	0.40	1.88	76.98	42.74	1.48	51.21	63.57	2.22	6.49	321.11	32.80	1389.23	117.52
	SHB44X	41.02	2.83	0.45	2.00	76.15	40.97	1.43	49.56	62.07	1.89	5.32	375.57	46.11	1666.36	169.08
	SHB4-14H	44.33	3.01	0.41	2.27	75.89	42.82	1.48	49.06	62.27	2.04	5.31	371.31	45.16	1643.00	170.07
	SHB4-5H	41.74	2.99	0.48	2.03	75.71	42.87	1.48	48.34	61.05	1.86	5.33	414.10	51.22	1876.77	185.79
	SHB4-9H	39.66	3.16	0.47	2.11	76.38	45.10	1.53	47.73	62.13	1.89	5.46	440.46	54.11	1945.96	190.91
	SHB4-6H	42.37	3.17	0.49	2.16	76.21	43.28	1.49	48.24	62.21	2.12	5.53	456.00	54.27	2026.42	194.45
	SHB4-11H	43.26	2.68	0.47	2.09	75.13	41.65	1.45	47.91	60.76	2.04	5.34	463.99	55.39	2118.46	208.17
north subsection	SHB4-4H	43.88	3.64	0.62	2.70	77.55	44.01	1.51	41.16	63.49	2.28	5.61	800.11	91.93	3485.61	334.58
	SHB4-2H	45.34	3.62	0.79	3.13	79.13	45.06	1.53	38.45	65.80	2.59	6.17	1117.43	116.45	4559.21	415.80
	SHB4-7H	42.34	3.44	0.79	2.90	78.91	45.29	1.54	39.95	64.70	2.32	5.86	1180.12	130.42	4963.67	462.25
	SHB4-8H	44.87	3.34	0.63	2.60	76.11	44.40	1.52	47.13	62.66	2.22	5.58	668.40	78.95	2883.39	276.69
	SHB46X	39.14	3.38	0.57	2.56	76.55	43.96	1.51	47.31	62.63	2.24	5.55	604.78	71.91	2582.74	254.21
	SHB4-12H	48.12	2.89	0.76	3.03	78.16	44.49	1.52	43.16	63.36	2.40	5.96	955.82	104.26	3952.35	370.93
	SHB42X	44.65	2.80	0.60	3.03	78.02	44.18	1.51	45.42	62.96	2.34	5.74	634.15	70.71	2529.25	251.42
	SHB4-3H	46.86	2.76	0.62	2.92	77.46	44.71	1.53	45.97	62.77	2.28	5.69	640.53	72.15	2558.42	256.68

[a]H = heptane value [H = (nC_7 × 100)/(CH + 2-MH + 2, 3-DMP + 1, 1-DMCP + 3-MH + 1c3-DMCP + 1t3-DMCP + 1t2-DMCP + nC_7 + MCH)]; I = isoheptane value [I = (2 + 3)-MH/(1c3 + 1t3 + 1t2)-DMCP]; B = Tol/nC_7; F = nC_7/MCH, MAI = 1-MA/(1-MA + 2-MA); MDI = 4-MD/(1-MD + 3-MD + 4-MD); Rc = 0.4389 + 0.0243MDI; EAI = 1-EA/(1-EA + 2-EA); DMAI-1 = 1, 3-DMA/(1, 2-DMA + 1, 3-DMA); A/D = adamantane/diamantane; MA/MD = methyladamantane/methyldiamantane; MA: methyladamantanes; MD: methyldiamantanes.

https://doi.org/10.1021/acs.energyfuels.4c02159
Energy Fuels 2024, 38, 18413−18430

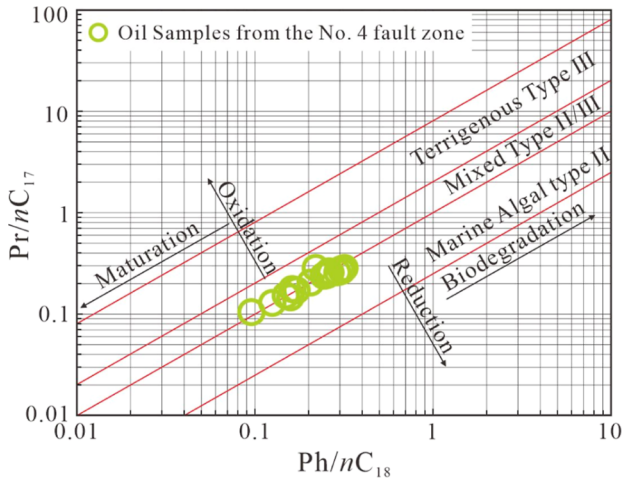

Figure 7. Cross-plots of phytane (Ph)/nC_{18} versus pristane (Pr)/nC_{17} to identify depositional environments (modified with permission from ref 73. Copyright 2018 American Chemical Society).

oil maturity of F4 south is higher than that of the north (Table 1).

Previous studies have suggested that as aromatic parameters approach the thermal evolution threshold, demethylation processes become dominant, resulting in parameter inversions.[8] This study utilizes the % Rc calculated by MDI as a standard to evaluate the application and limitation of various aromatic parameters in high-maturity oil from ultradeep reservoirs.

5.3. Application and Limitation of Aromatic Maturity Parameters. *5.3.1. Phenanthrene Homologues.* Figure 13 illustrates the relationship among MPI-1, MPI-2, F1 [F1 = (2-MP + 3-MP)/(2-MP + 3-MP + 9-MP + 1-MP)], F2 [F2 = 2-MP/(3-MP + 2-MP + 1-MP + 9-MP)], and Rc, revealing consistent trends. A strong positive correlation between Rc and these parameters occurs when Rc < 1.48%. Moreover, the correlation coefficient reaches as high as 0.92 between MPI-1 and Rc (Figure 13 and Table 4). But when Rc > 1.48%, all parameters began to have a certain negative correlation with Rc (Figure 13). Previous studies indicate that methylation, isomerization, and demethylation processes assume different dominant roles at various thermal maturity levels.[35] Isomerization and methylation dominate during stages of comparatively low thermal maturity. Demethylation was dominant in the highly mature stage, and as maturity increased, the relevant maturity parameters decreased.

In combination with the F4 oils, it was observed that when Rc < 1.48%, methylation and methyl rearrangement play dominant roles among phenanthrene homologues. Methylation leads to the formation of 2-MP and 3-MP from phenanthrene, while unstable α-substituent isomers (9-MP and 1-MP) gradually transform into stable β-substituent isomers (3-MP and 2-MP) (Figure 14). There was a positive correlation between the maturity parameters of phenanthrene homologues and Rc. When Rc > 1.48%, the demethylation process was dominant. At this time, the content of phenanthrene compounds gradually increased, resulting in the relative maturity parameters beginning to decrease and reverse (Figure 14). Radke and Welte (1983) concluded that when Ro > 1.35%, the MPI-1 value would "reverse".[8] This is inconsistent with the results observed in samples from the study area (Rc > 1.48%). This difference may be primarily due to regional geological factors (e.g., sedimentary facies, geothermal gradient, and organic matter source). Therefore, when the oil maturity in the Shunbei oilfield is below 1.48%, methylphenanthrene maturity parameters such as MPI-1, MPI-2, F1, and F2 can reliably assess oil maturity.

5.3.2. Dibenzothiophene Homologues. Dibenzothiophene compounds can be formed by secondary processes, such as TSR, in addition to sulfur incorporation during deposition and diagenetic sulfurization at low temperatures.[57] Studies have shown that the Ordovician strata in the Shunbei oilfield lack salt-rock layers, making them unsuitable for TSR.[47] Moreover, the concentration of dibenzothiophene compounds in the Shunbei oilfield is significantly lower compared to TSR oil in the Tarim Basin.[58] Consequently, TSR does not significantly affect the dibenzothiophene compounds in the F4 oil.

Based on Rc, we analyzed the application of maturity parameters of dibenzothiophene series [4-/1-MDBT, 2, 4-/(1, 6- + 1, 4-DMDBT), and 4, 6-/(1, 6- + 1, 4-DMDBT)]. It is found that the variation of these parameters is consistent with phenanthrene homologues, and "inversion" occurs at Rc = 1.48%. When Rc < 1.48%, the dibenzothiophene homologue parameters exhibit a strong positive correlation with Rc ($R^2 \geq 0.82$) (Figure 15; Table 4). This suggests that the relevant dibenzothiophene parameters can reliably assess the maturity of F4 oils at Rc < 1.48%. Conversely, when Rc > 1.48%, the

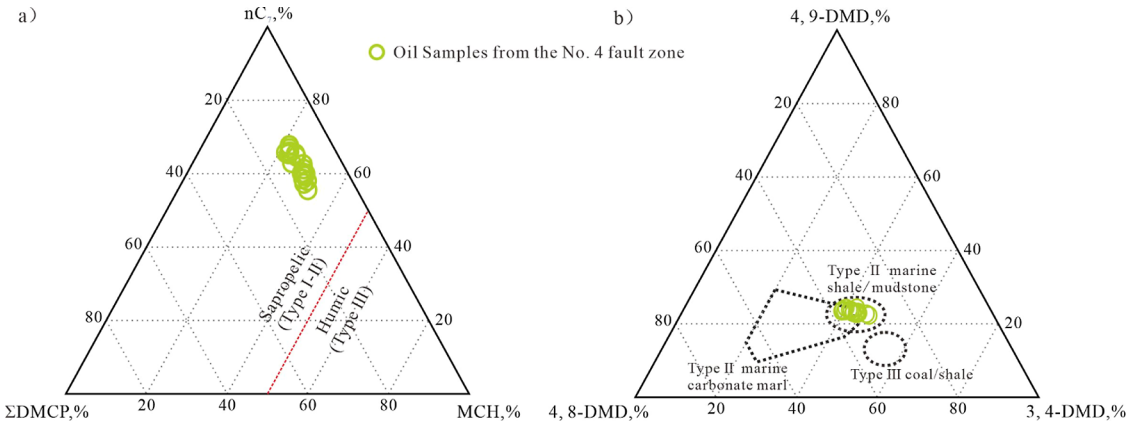

Figure 8. Triangle diagram derived from light hydrocarbons and diamondoids indicating the organic input and depositional environment. (a) nC_7, ΣDMCP, and MCH (modified with permission from ref 74. Copyright 2021 American Chemical Society); (b) 4,9-DMD; 4,8-DMD; and 3,4-DMD (modified with permission from ref 31. Copyright 2001 Elsevier).

https://doi.org/10.1021/acs.energyfuels.4c02159
Energy Fuels 2024, 38, 18413−18430

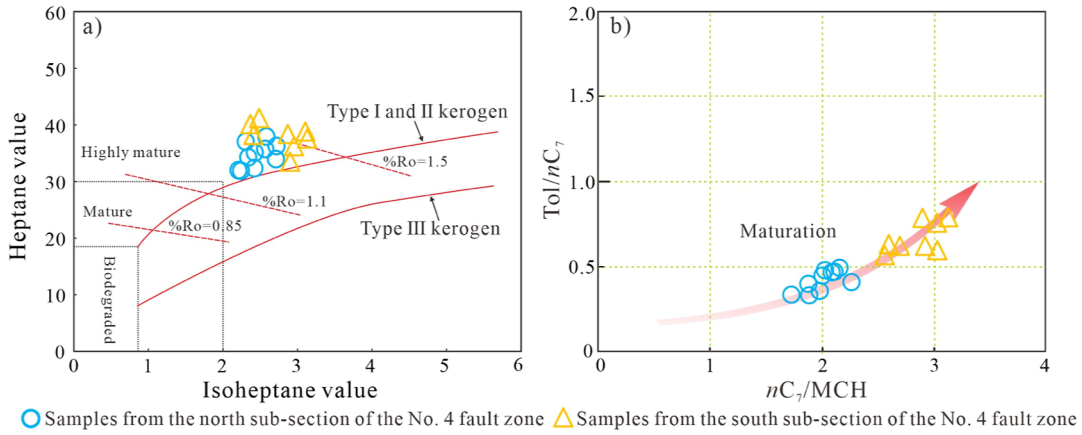

Figure 9. Light hydrocarbon parameters identify the maturity of the oils in the Shunbei oilfield. (a) Heptane value (H) versus isoheptane value (I) (modified with permission from ref 74. Copyright 2021 American Chemical Society); (b) Tol/nC_7 versus nC_7/MCH (modified with permission from ref 53. Copyright 1987 Elsevier Ltd.).

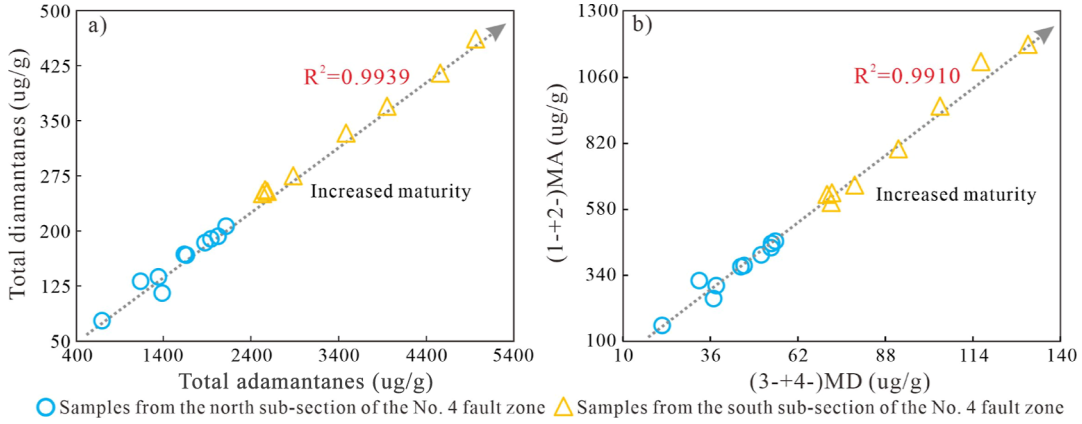

Figure 10. Cross-plots of (a) total adamantanes versus total diamantanes and (b) concentrations of (3 + 4)-MD versus (1 + 2)-MA.

dibenzothiophene homologue parameters showed a consistent decline.

The mass chromatographic characteristics of m/z 198 showed that the decrease of the 4-/1-MDBT ratio was mainly caused by the increase of the relative content of 1-MDBT (Figure 16). Previous studies have found that 4-MDBT has higher thermodynamic stability than 1-MDBT through molecular dynamics analysis. Moreover, 1-MDBT will continuously transform into 4-MDBT in the process of thermal evolution.[59,60] However, most simulation experiments found that the 4-/1-MDBT ratio would change from monotonically increasing to monotonically decreasing in the high maturity stage.[61] For example, Wu et al. (2019) conducted a closed thermal simulation experiment on methyldibenzothiophene and observed that when the thermal simulation temperature reached 400 °C (easy % Ro = 1.49%), the 4-/1-MDBT ratio began to monotonically decrease.[61] This may be due to differences in experimental systems and geological conditions. Specifically, the traditional simulation experiment is carried out by the principle of temperature−time compensation. The reaction system under the control and influence of this thermodynamic property cannot satisfy the time required to reach kinetic equilibrium. Therefore, 1-MDBT is generated preferentially rather than 4-MDBT. Quantitative tests show that the "reversal" of MDR in oil from the Shunbei oilfield is also caused by the decrease of 4-MDBT content and the increase of 1-MDBT content (Figure 16). This coincides closely with the results of the laboratory simulations. In addition, previous studies have suggested that large-scale magmatic activity occurred in the Late Permian in Shunbei area.[62] This transient rapid heating of short aging may be the specific reason for the "inversion" of 4-/1-MDBT ratio in the study area.

5.3.3. Naphthalene Homologues. Naphthalene homologues are often detected and reported in source rocks and crude oil from various basins in the world.[63−65] Naphthalene, comprising two benzene rings sharing two carbon atoms, exhibits higher thermal stability at the β position due to greater steric hindrance and electron cloud density compared to those at the α position. Consequently, the ratio of β-substituted to α-substituted naphthalene isomers can serve as a maturity indicator.[15] For example, methyl naphthalene (MNR, MNR = 2-/1-MN), dimethyl naphthalene [DNR, DNR = (2, 7- + 2, 6-)/1, 5-DMN], trimethyl naphthalene (TMNr), tetramethylnaphthalene (TeMNr), and pentamethylnaphthalene [PMNr, PMNr = 1, 2, 4, 6, 7-/(1, 2, 4, 6, 7- + 1, 2, 3, 5, 6-)-PMN] can be used to assess maturity and widely used in various basins worldwide.[66−68]

As shown in Figure 17, the MNR and DNR are negatively correlated with Rc. Previous studies suggested that under the influence of thermally induced condensation of aromatic hydrocarbons, MNR and DNR values were reversed at about 1.1% Ro.[35] It is worth noting that MNR and DNR enter the "inversion" threshold significantly earlier than the maturity index of phenanthrene and dibenzothiophene series com-

https://doi.org/10.1021/acs.energyfuels.4c02159
Energy Fuels 2024, 38, 18413−18430

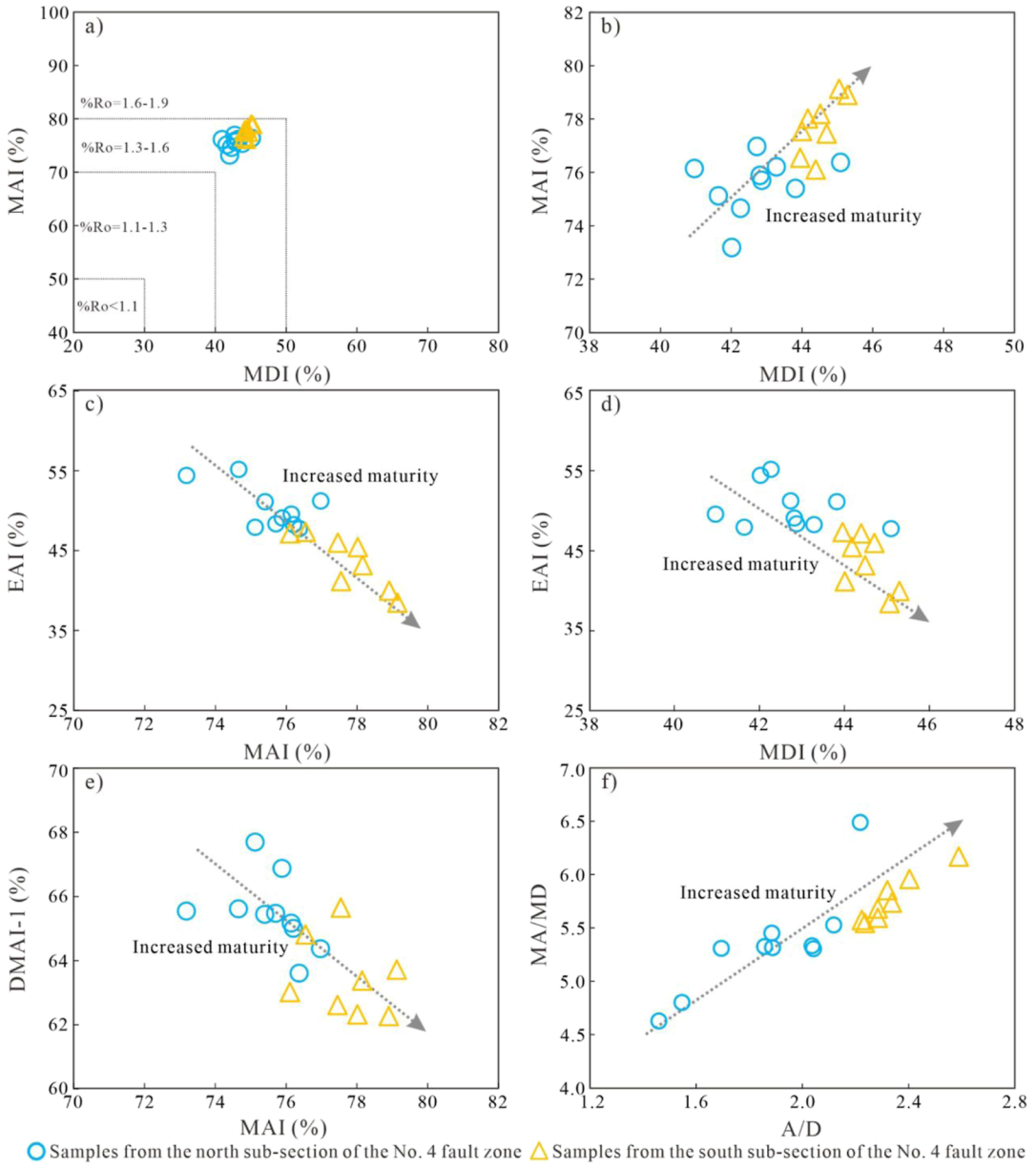

Figure 11. Diamondoid parameters identify the maturity of the oils. (a,b) MAI versus MDI (modified with permission from ref 28. Copyright 1996 Elsevier); (c) EAI versus MAI; (d) EAI versus MDI; (e) DMAI-1 versus MAI; (f) MA/MD versus A/D.

pounds, which may be due to thermally induced condensation of aromatic hydrocarbons.[35] The Rc of oil in the study area generally exceeded 1.42%, which results in a negative correlation of both the MNR and DNR with Rc, respectively. In addition, TMNr and TeMNr have no obvious correlation with Rc, suggesting their potential unsuitability for maturity evaluation in the Shunbei oilfield (Figure 17 and Table 4).

Previous studies suggest that methyl rearrangement between pentamethylnaphthalene series compounds occurs at early maturation stages.[64] However, the low content of this compound series in maturity stages may not effectively indicate thermal evolution maturity.[35] From this study, we deduce that methyl rearrangement between pentamethylnaphthalene series compounds occurs extensively in high thermal evolution stages, suitable for maturity evaluation only in crude oil or source rock at this stage.[69] PMNr parameters in the oil exhibit a robust positive correlation with Rc ($R^2 = 0.78$) (Figure 18 and Table 4). Additionally, GOR, nC_7/MCH, and (3 + 4)-MD (μg/g) also demonstrate a strong positive correlation with PMNr (Figure 18). Based on hydrocarbon property analysis, various maturity parameters (light hydrocarbons and diamondoids), and the synthesis mechanism of pentamethylnaphthalene series compounds, PMNr parameters can serve as maturity indices for highly mature oil. Moreover, Wang et al. (2021) successfully employed PMNr to assess the maturity of F1 and F5 crude oils in the Shunbei oilfield, indicating its applicability to maturity evaluation in this oilfield.[15]

5.3.4. Aromatic Maturity Parameters. With increasing global industrial demand, petroleum exploration is increasingly focusing on ultradeep reservoirs. The Shunbei oilfield exemplifies ultradeep petroleum exploration, with a Paleozoic reservoir depth ranging from 7300 to 10,000 m. Applying aromatic parameters to evaluate oil maturity in the Shunbei oilfield offers valuable insights for ultradeep petroleum exploration globally.

https://doi.org/10.1021/acs.energyfuels.4c02159
Energy Fuels 2024, 38, 18413−18430

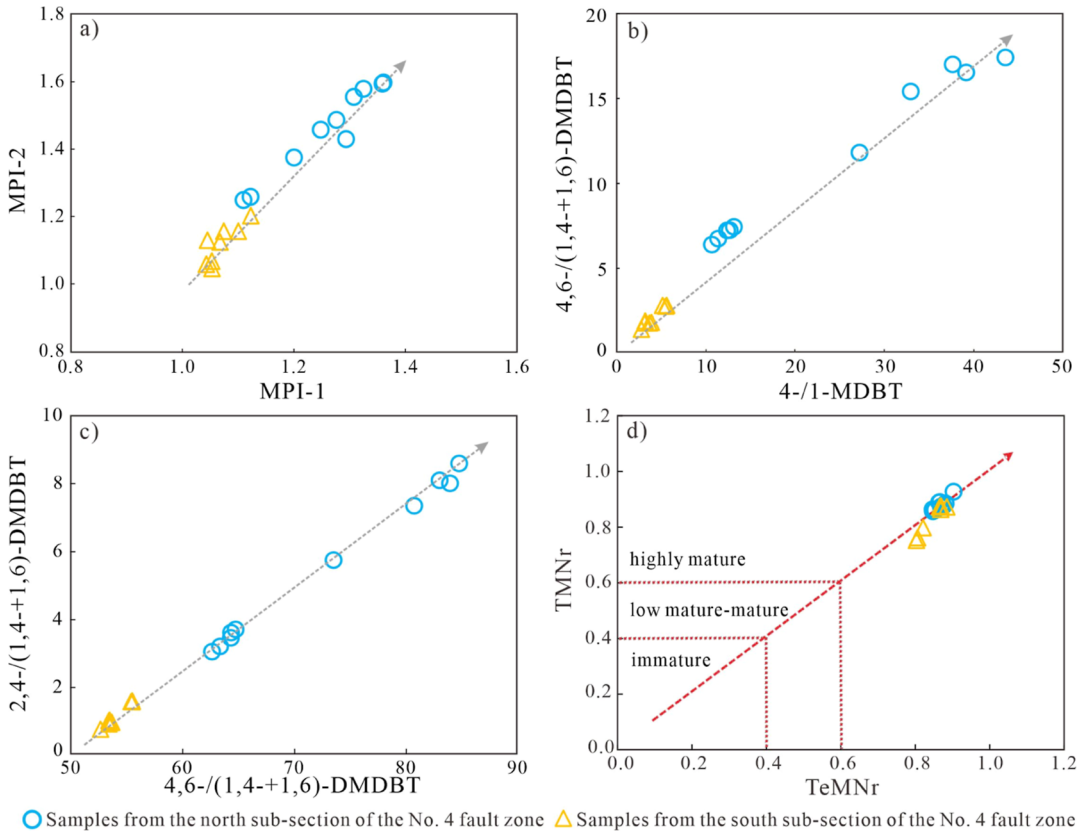

Figure 12. Aromatic hydrocarbon parameters identify the maturity of the oils. (a) MPI-2 versus MPI-1; (b) 4, 6-/(1, 4- + 1, 6-)DMDBT versus 4-/1-MDBT; (c) 2, 4-/(1, 4- + 1, 6-)DMDBT versus 4, 6-/(1, 4- + 1, 6-)DMDBT; (d) TMNr versus TeMNr.

Table 4. Aromatic Hydrocarbon Maturity Parameters of the Shunbei Oil[a]

area	well	MNR	DNR	TMNr	TeMNr	PMNr	MPI-1	MPI-2	4-/1-MDBT	2, 4-/(1, 4- + 1, 6-) DMDBT	4, 6-/(1, 4- + 1, 6-) DMDBT
south subsection	MS3	2.70	12.88	0.86	0.85	0.56	1.32	1.58	32.98	7.34	15.41
	MS1	2.50	12.17	0.86	0.85	0.61	1.31	1.55	37.69	8.00	17.02
	MS4	2.97	14.70	0.89	0.87	0.65	1.36	1.59	43.60	8.58	17.42
	SHB4-10H	2.95	14.58	0.89	0.86	0.63	1.36	1.60	39.20	8.09	16.54
	SHB44X	2.46	10.96	0.85	0.85	0.57	1.28	1.49	13.14	3.68	7.39
	SHB4-14H	2.45	11.00	0.86	0.85	0.58	1.25	1.46	12.67	3.59	7.19
	SHB4-5H	2.30	10.29	0.88	0.88	0.65	1.20	1.37	12.39	3.43	7.18
	SHB4-9H	2.20	9.47	0.87	0.88	0.62	1.11	1.25	11.37	3.18	6.70
	SHB4-6H	2.21	9.53	0.87	0.87	0.61	1.12	1.26	10.68	3.02	6.34
	SHB4-11H	3.01	17.14	0.92	0.90	0.74	1.29	1.43	27.24	5.73	11.78
north subsection	SHB4-4H	2.49	10.76	0.87	0.87	0.66	1.12	1.20	5.12	1.54	2.75
	SHB4-2H	2.26	8.61	0.86	0.87	0.70	1.04	1.06	3.65	0.98	1.70
	SHB4-7H	2.30	8.88	0.87	0.88	0.73	1.05	1.07	3.87	1.00	1.74
	SHB4-8H	2.36	10.26	0.87	0.87	0.67	1.10	1.16	5.58	1.57	2.75
	SHB46X	2.37	10.19	0.87	0.86	0.67	1.07	1.13	5.47	1.54	2.70
	SHB4-12H	2.34	7.92	0.80	0.82	0.68	1.05	1.05	2.74	0.73	1.33
	SHB42X	1.93	6.07	0.76	0.81	0.65	1.07	1.16	3.10	0.88	1.70
	SHB4-3H	1.93	6.05	0.75	0.80	0.66	1.04	1.13	3.17	0.93	1.83

[a]MNR = 2-/1-MN; DNR = (2, 6- + 2, 7-)/1, 5-DMN; TMNr = 1, 3, 7-/(1, 3, 7- + 1, 2, 5-)TMN; TeMNr = 1, 3, 6, 7-/(1, 3, 6, 7 + 1, 2, 5, 6 + 1, 2, 3, 5)-TeMN; PMNr = 1, 2, 4, 6, 7-/(1, 2, 4, 6, 7 + 1, 2, 3, 5, 6)-PMN; MPI-1 = 1.5 × (2-MP + 3-MP)/(P + 1-MP + 9-MP); MPI-2 = 3 × (2-MP)/(P + 1-MP + 9-MP).

The results indicate that most aromatic maturity parameters have significant limitations in evaluating highly mature oil. Phenanthrene, dibenzothiophene, and methylnaphthalene (including MNR and DNR) parameters reach the "inverted" threshold at Rc values of 1.48%, 1.48%, and 1.10%, respectively.[35] The maturity parameter remains effective for evaluating oil maturity below the "inversion" threshold. Previous studies indicate that diamondoid maturity parameters are

https://doi.org/10.1021/acs.energyfuels.4c02159
Energy Fuels 2024, 38, 18413−18430

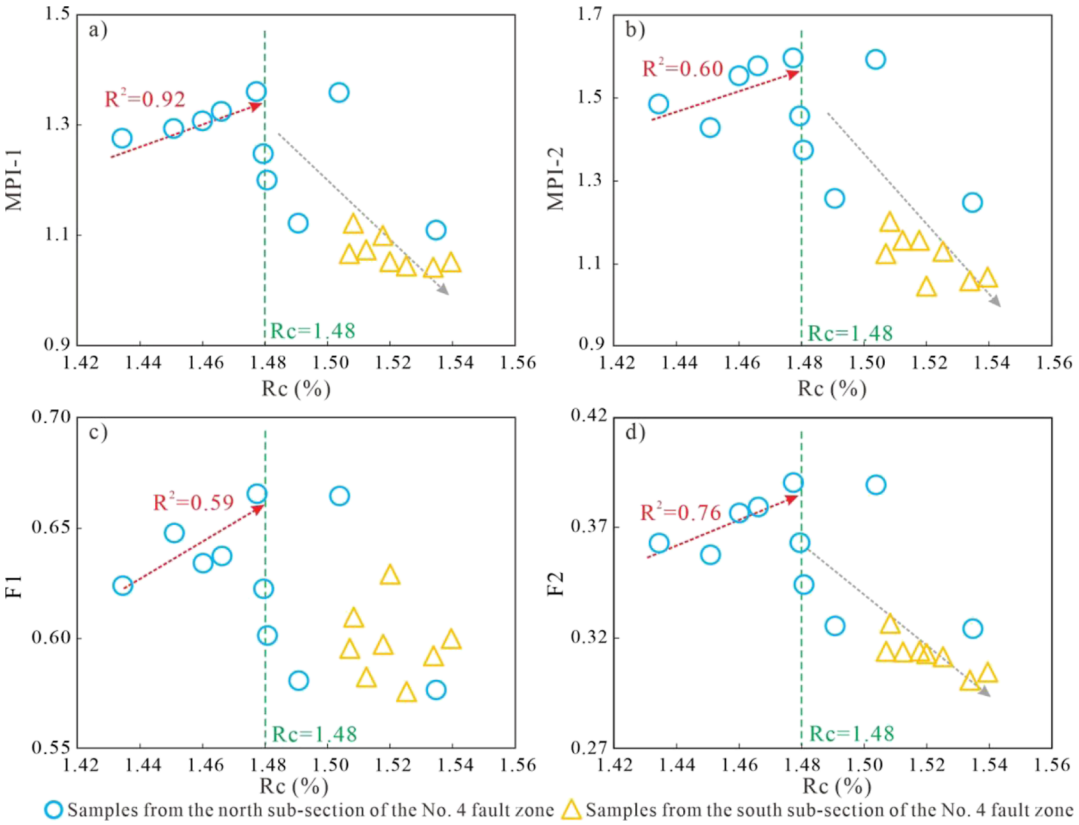

Figure 13. Cross-plots of the phenanthrene parameters versus Rc (%). (a) MPI-1 versus Rc (%); (b) MPI-2 versus Rc (%); (c) F1 versus Rc (%); (d) F2 versus Rc (%). (% Rc = 0.0243MDI + 0.4389).

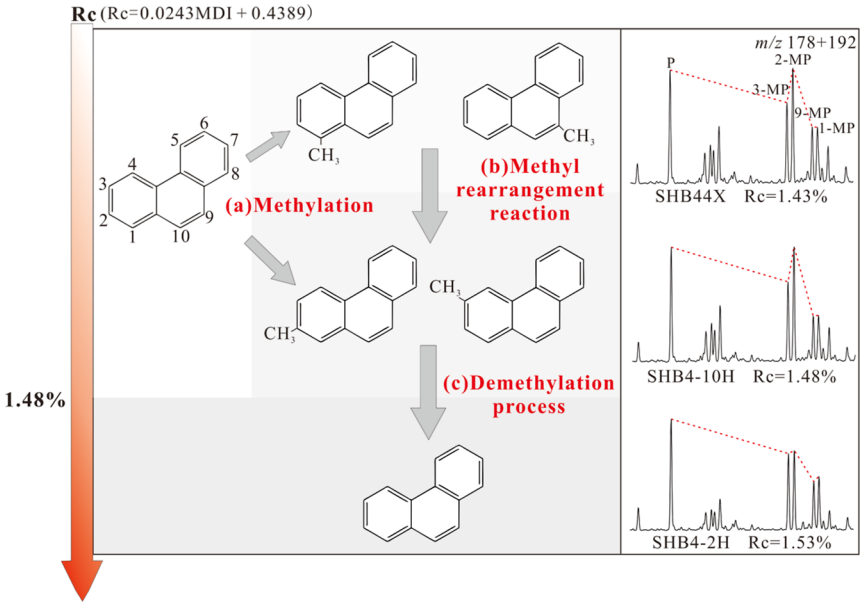

Figure 14. Schematic diagram of methylphenanthrene isomer transformation.

applicable across a wide range of thermal evolutions. However, most studies believe that it has better applicability in the high maturity stage (Rc > 1.3%).[70−72] Additionally, the study indicates that PMNr effectively characterizes the maturity of highly mature oil in the Shunbei oilfield. Previous studies have shown significant limitations in the application of PMNr during the early thermal evolution stage. However, for highly mature oil in ultradeep reservoirs, PMNr remains a reliable maturity index. Comprehensive analysis indicates that aromatic parameters remain essential in evaluating the oil maturity at various stages of thermal evolution.

6. CONCLUSIONS

In summary, our investigation of the no. 4 fault zone (F4) in the Shunbei oilfield indicates a predominance of condensate reservoirs with only two volatile reservoirs (MS1 and MS3)

https://doi.org/10.1021/acs.energyfuels.4c02159
Energy Fuels 2024, 38, 18413−18430

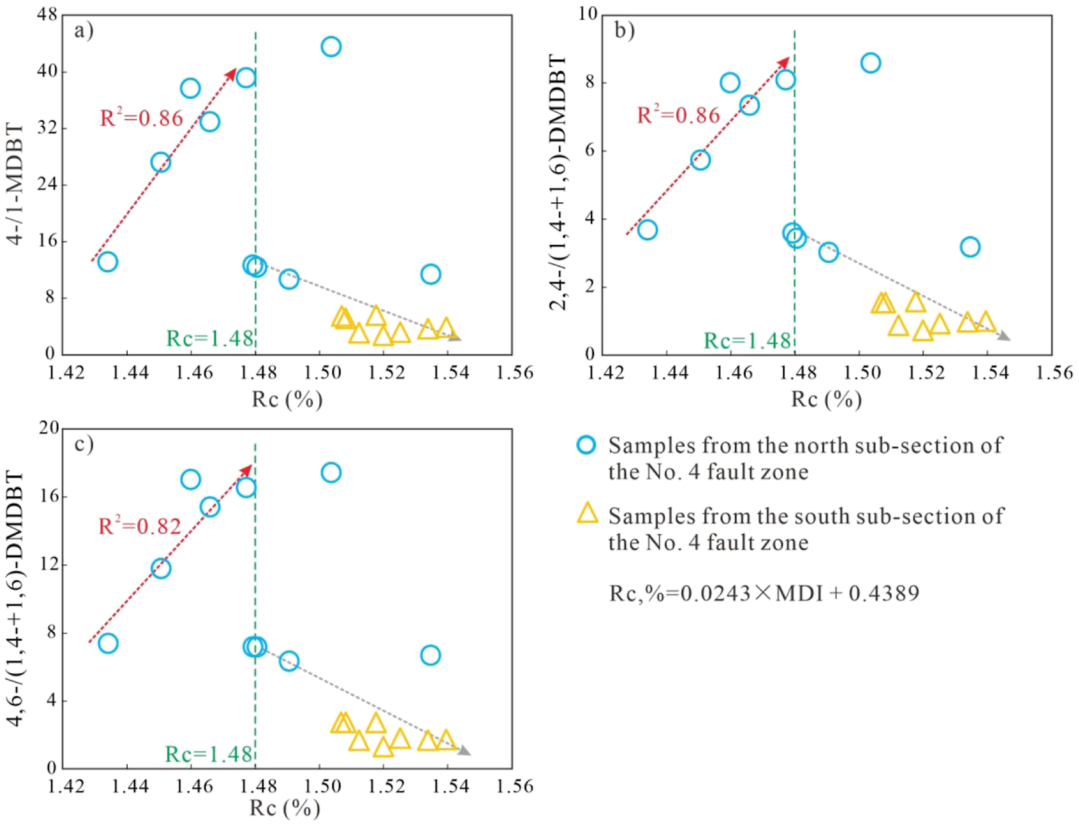

Figure 15. Cross-plots of the dibenzothiophene parameters versus Rc (%). (a) 4-/1-MDBT versus Rc (%); (b) 2, 4-/(1, 4- + 1, 6-)DMDBT versus Rc (%); (c) 4, 6-/(1, 4- + 1, 6-)DMDBT versus Rc (%).

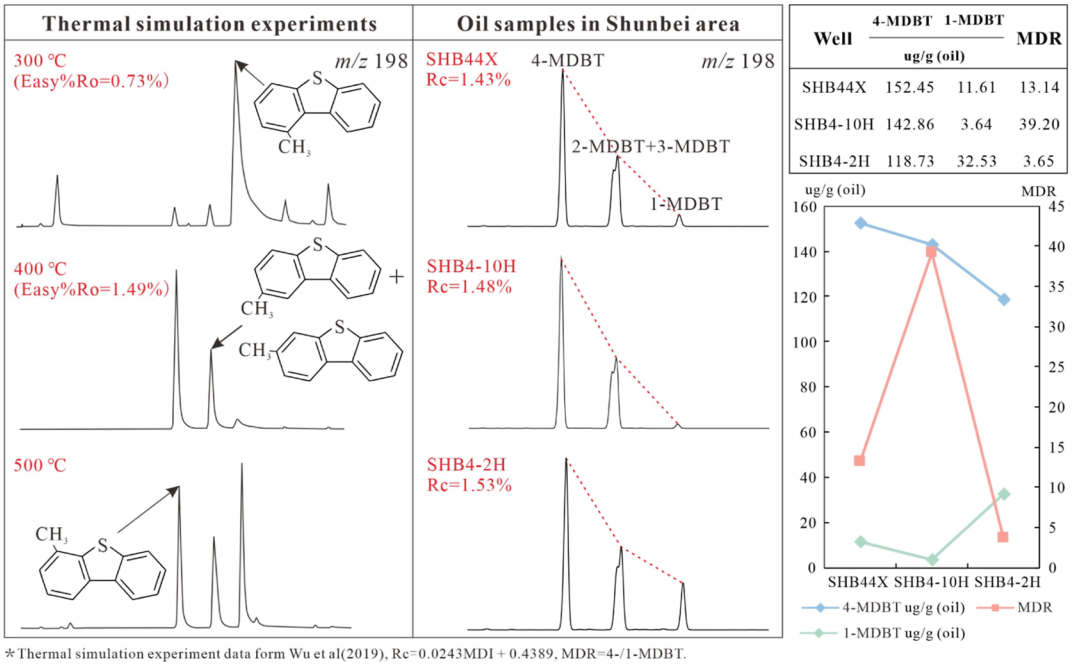

*Thermal simulation experiment data form Wu et al(2019), Rc=0.0243MDI + 0.4389, MDR=4-/1-MDBT.

Figure 16. Mass chromatogram (m/z 198) and content distribution of MDBTs at different maturities (data of thermal simulation experiment from ref 61).

observed in the northernmost part of the fault zone. The oils are from the same source kitchen, which are formed from a reduced depositional environment and sourced from marine type II organic matter.

Analysis using GC and GC−MS revealed significant saturation hydrocarbon cracking in F4 oils with well-preserved aromatic hydrocarbons. Moreover, F4 oils contain abundant light hydrocarbons and diamondoid compounds. Maturation parameters of light hydrocarbons and diamondoids suggest high

https://doi.org/10.1021/acs.energyfuels.4c02159
Energy Fuels 2024, 38, 18413−18430

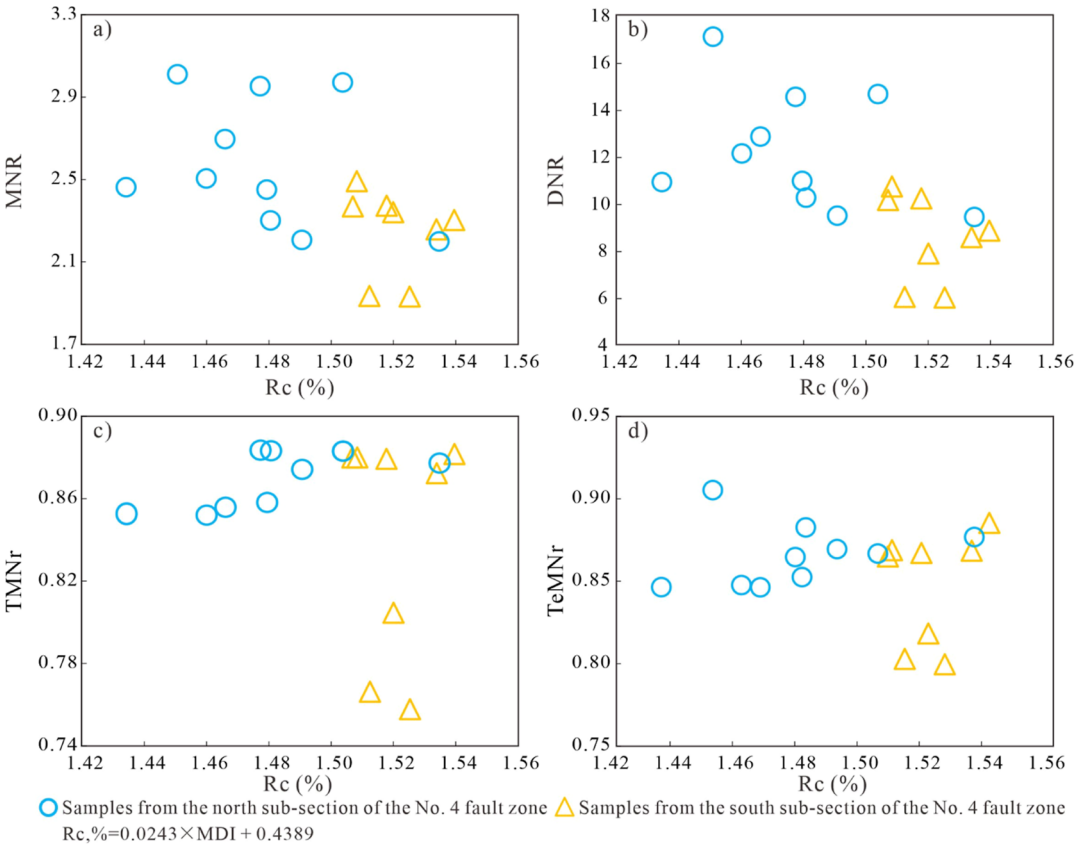

Figure 17. Cross-plots of the naphthalenes parameters versus Rc (%). (a) MNR versus Rc (%); (b) DNR versus Rc (%); (c) TMNr versus Rc (%); (d) TeMNr versus Rc (%).

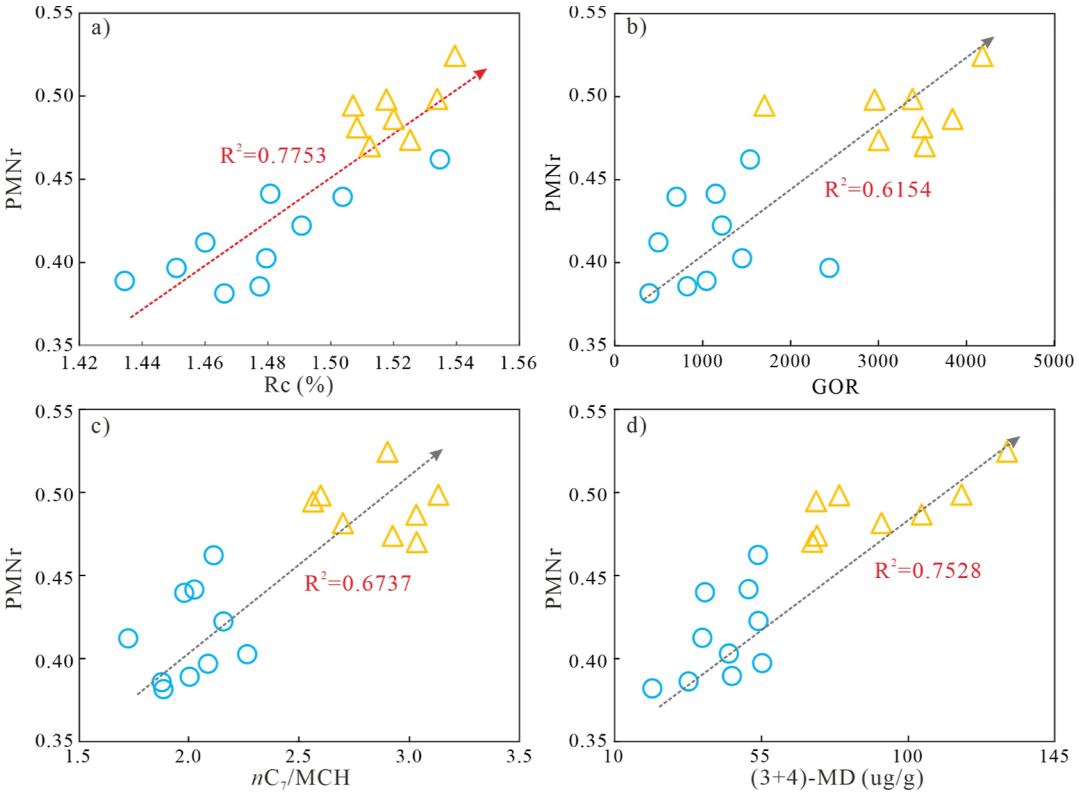

Figure 18. Cross-plots of (a) PMNr versus Rc (%); (b) PMNr versus GOR; (c) PMNr versus nC_7/MCH; (d) PMNr versus (3 + 4)-MD.

https://doi.org/10.1021/acs.energyfuels.4c02159
Energy Fuels 2024, 38, 18413−18430

thermal evolution in F4 oils, with % Rc (% Rc = 0.0243MDI + 0.4389) ranging from 1.43% to 1.54%. Interestingly, aromatic hydrocarbon parameters exhibited contrasting trends compared to light hydrocarbon and diamondoid maturity parameters.

The majority of aromatic maturity parameters present significant limitations at the high thermal evolution stages. Specifically, phenanthrene (MPI-1, MPI-2, F1, and F2) and dibenzothiophene [4-/1-MDBT; 2, 4-/(1, 4- + 1, 6-)DMDBT; and 4, 6-/(1, 4- + 1, 6-)DMDBT] parameters undergo "reversal" due to demethylation and thermal alteration, respectively. Moreover, most naphthalene maturity parameters (MNR and DNR) are influenced by thermally induced condensation, making them unsuitable for maturity assessment in highly mature oil. TMNr and TeMNr exhibit little significant correlation with Rc and may not be appropriate for maturity evaluation in the study area. However, PMNr demonstrates a robust positive correlation with GOR, nC_7/MCH, and (3 + 4)-MD concentrations, suggesting their efficacy as maturity indicators at high thermal evolution stages.

Caution should be exercised in the application of aromatic maturity parameters in ultradeep basins such as the Tarim Basin.

AUTHOR INFORMATION

Corresponding Author

Meijun Li − *National Key Laboratory of Petroleum Resources and Engineering, College of Geosciences, China University of Petroleum (Beijing), Beijing 102249, China;* orcid.org/0000-0002-7141-6068; Email: meijunli@cup.edu.cn

Authors

Donglin Zhang − *National Key Laboratory of Petroleum Resources and Engineering, College of Geosciences, China University of Petroleum (Beijing), Beijing 102249, China*

Rongzhen Qiao − *National Key Laboratory of Petroleum Resources and Engineering, College of Geosciences, China University of Petroleum (Beijing), Beijing 102249, China*

Hong Xiao − *National Key Laboratory of Petroleum Resources and Engineering, College of Geosciences, China University of Petroleum (Beijing), Beijing 102249, China*

Complete contact information is available at: https://pubs.acs.org/10.1021/acs.energyfuels.4c02159

Notes

The authors declare no competing financial interest.

ACKNOWLEDGMENTS

This work was funded by the National Natural Science Foundation of China (grant no. 42173054). The authors gratefully acknowledge the SINOPEC Northwest Company (Urumqi) for sample collection.

REFERENCES

(1) Mackenzie, A. S.; Patience, R. L.; Yon, D. A.; Maxwell, J. R. The effect of maturation on the configurations of acyclic isoprenoid acids in sediments. *Geochim. Cosmochim. Acta* **1982**, *46* (5), 783−792.

(2) Fu, J.; Li, M. J.; Sun, Y. G.; Li, Y. C.; Yang, Y. C.; Lu, X. L.; Lai, G. T. Thermal maturity of crude oils in the Baiyun sag, Pearl River Mouth basin, South China Sea: Insights from biomarkers, aromatic hydrocarbon and adamantane compounds. *Mar. Pet. Geol.* **2023**, *155*, 106353.

(3) Mccabe, L. C.; Quirke, T. T. *Angle of Polarization as an Index of Coal Rank*; The American Institute of Mining, Metallurgical, and Petroleum Engineers, Technol. Publ., 1937; Vol. *791*, p 11.

(4) Dutcher, R. R.; Hacquebard, P. A.; Schopf, J. M.; Simon, J. A. Carbonaceous materials as indicators of metamorphism. *Special Papers | Geological Society of America*; GeoScienceWorld, 1974; Vol. *153*, p 116.

(5) Pawlewicz, M. J.; King, D. J. Vitrinite and solid bitumen reflectance: some correlations and applications. *The Petroleum System−Status of Research and Methods*; Magoon, L. B., Ed.; U.S. Geological Survery Bulletin, 1992; pp 58−60.

(6) Teichmuller, M.; Wolf, M. Application of fluorescence microscopy in coal petrology and oil exploration. *J. Microsc.* **1977**, *109* (1), 49−73.

(7) Buchardt, B.; Lewan, M. D. Reflectance of vitrinite-like macerals as a thermal maturity index for Cambrian-Ordovician Alum Shale, Southern Scandinavia. *AAPG Bull.* **1990**, *74* (4), 394−406.

(8) Radke, M.; Welte, D. H. The Methylphenanthrene Index (MPI): A Maturity Parameter Based on Aromatic Hydrocarbons. *Advances in Organic Geochemistry*; Bjoroy, M., et al., Eds; Wiley: New York, 1983, pp 504−512.

(9) Alexander, R.; Kagi, R. I.; Rowland, S. J.; Sheppard, P. N.; Chirila, T. V. The effects of thermal maturity on distributions of dimethylnaphthalenes and trimethylnaphthalenes in some ancient sediments and petroleums. *Geochim. Cosmochim. Acta* **1985**, *49* (2), 385−395.

(10) Peters, K. E.; Moldowan, J. M. *The Biomarker Guide: Interpreting Molecular Fossils in Petroleum and Ancient Sediments*; Prentice Hall: NJ, 1993.

(11) Oldenburg, T. B. P.; Brown, M.; Bennett, B.; Larter, S. R. The impact of thermal maturity level on the composition of crude oils, assessed using ultra-high resolution mass spectrometry. *Org. Geochem.* **2014**, *75*, 151−168.

(12) Farrimond, P.; Taylor, A.; TelnÆs, N. Biomarker maturity parameters: The role of generation and thermal degradation. *Org. Geochem.* **1998**, *29* (5−7), 1181−1197.

(13) Wilhelms, A.; Larter, S. Shaken but not always stirred. Impact of petroleum charge mixing on reservoir geochemistry. *Understanding Petroleum Reservoirs: towards an Integrated Reservoir Engineering and Geochemical Approach*; Geological Society Special Publication, 2004; Vol. *237*, pp 27−35.

(14) Radke, M. Application of aromatic compounds as maturity indicators in source rocks and crude oils. *Mar. Pet. Geol.* **1988**, *5*, 224−236.

(15) Wang, Q.; Hao, F.; Cao, Z. C.; Tian, J. Q.; Cong, F. Y. Geochemistry and origin of the ultra-deep Ordovician oils in the Shunbei field, Tarim Basin, China: Implications on alteration and mixing. *Mar. Pet. Geol.* **2021**, *123*, 104725.

(16) Srinivasan, P.; Jacobi, D.; Arguello, E. M. E.; Atwah, I.; Karg, H.; Azzouni, A. Thermal maturity calculation in Type II-S source rocks using the alkyl dibenzothiophenes. *Org. Geochem.* **2023**, *185*, 104676.

(17) Radke, M.; Welte, D. H.; Willsch, H. Maturity parameters based on aromatic hydrocarbons: Influence of the organic matter type. *Org. Geochem.* **1986**, *10* (1−3), 51−63.

(18) Budzinski, H.; Garrigues, P.; Connan, J.; Devillers, J.; Domine, D.; Radke, M.; Oudins, J. Alkylated phenanthrene distributions as maturity and origin indicators in crude oils and rock extracts. *Geochim. Cosmochim. Acta* **1995**, *59* (10), 2043−2056.

(19) Chakhmakhchev, A.; Suzuki, M.; Takayama, K. Distribution of alkylated dibenzothiophenes in petroleum as a tool for maturity assessments. *Org. Geochem.* **1997**, *26* (7−8), 483−489.

(20) Peters, K. E.; Walters, C. C.; Moldowan, J. M. *The Biomarker Guide: Biomarkers and Isotopes in the Petroleum Exploration and Earth History*, 2nd ed.; Cambridge University Press: New York, 2005.

(21) Hunt, J. M.; Huc, A. Y.; Whelan, J. K. Generation of light hydrocarbons in sedimentary rocks. *Nature* **1980**, *288*, 688−690.

(22) Wang, P. R.; Xu, G. J.; Xiao, T. R.; Zhang, D. J.; Zhang, B. Application of C_5−C_{13} light hydrocarbons in depositional environment diagnosis. *Prog. Nat. Sci.* **2008**, *18* (9), 1129−1137.

(23) Thompson, K. F. M. Light hydrocarbons in subsurface sediments. *Geochim. Cosmochim. Acta* **1979**, *43* (5), 657−672.

(24) Mango, F. D. An invariance in the isoheptanes of petroleum. *Science* **1987**, *237* (4814), 514−517.

(25) Hou, D.; Wang, P.; Lin, R.; Li, S. Light Hydrocarbons in pyrolysis gas of maoming oil shale and its thermal evolution significance. *J. Jianghan Petroleum Inst.* **1989**, *11* (4), 7−11.
(26) Chen, X. H.; Zhang, M.; Huang, G. H.; Hu, G. Y.; Wang, X.; Xu, G. J. Geochemical characteristics of light hydrocarbons in cracking gases from chloroform bitumen A, crude oil and its fractions. *Sci. China, Ser. D: Earth Sci.* **2009**, *52*, 26−33.
(27) Wang, R. L.; Zhu, G. Y.; Wang, T.; Wen, Z. G.; Zhu, Y. Q.; Zhang, Z. Y. Identification of New Higher Diamondoids in Condensate, Their Elution Patterns, and Mechanisms: A Case Study from Well ZS1C, Tarim Basin. *Energy Fuels* **2024**, *38* (15), 14009−14024.
(28) Chen, J. H.; Fu, J. M.; Sheng, G. Y.; Liu, D. H.; Zhang, J. J. Diamondoid hydrocarbon ratios: novel maturity indices for highly mature crude oils. *Org. Geochem.* **1996**, *25* (3−4), 179−190.
(29) Gentzis, T.; Carvajal-Ortiz, H. Comparative study of conventional maturity proxies with the methyldiamondoid ratio: Examples from West Texas, the Middle East, and northern South America. *Int. J. Coal Geol.* **2018**, *197*, 115−125.
(30) Qiao, R. Z.; Chen, Z. H. Petroleum phase evolution at high temperature: A combined study of oil cracking experiment and deep oil in Dongying Depression, eastern China. *Fuel* **2022**, *326* (7), 124978.
(31) Schulz, L. K.; Wilhelms, A.; Rein, E.; Steen, A. S. Application of diamondoids to distinguish source rock facies. *Org. Geochem.* **2001**, *32* (3), 365−375.
(32) Zhang, S. C.; Huang, H. P.; Xiao, Z. Y.; Liang, D. G. Geochemistry of Palaeozoic marine petroleum from the Tarim Basin, NW China. Part 2: Maturity assessment. *Org. Geochem.* **2005**, *36* (8), 1215−1225.
(33) Wang, D. W.; Cai, C. F.; Yun, L.; Liu, J. Y.; Sun, P.; Jiang, Z. W.; Peng, Y. Y.; Zhang, H.; Wei, T. Y.; Pei, B. B. Controls on petroleum stability in deep and hot reservoirs: A case study from the Tarim Basin. *Mar. Pet. Geol.* **2023**, *147*, 106014.
(34) Dyman, T. S.; Crovelli, R. A.; Bartberger, C. E.; Takahashi, K. I. Worldwide estimates of deep natural gas resources based on the U.S. Geological Survey World Petroleum Assessment. *Nat. Resour. Res.* **2002**, *11*, 207−218.
(35) Wang, Q. R.; Huang, H. P.; He, C.; Li, Z. X.; Zheng, L. J. Methylation and demethylation of naphthalene homologs in highly thermal mature sediments. *Org. Geochem.* **2022**, *163*, 104343.
(36) Chen, Z. H.; Chai, Z.; Cheng, B.; Liu, H.; Cao, Y. C.; Cao, Z. C.; Qu, J. X. Geochemistry of high-maturity crude oil and gas from deep reservoirs and their geological significance: A case study on Shuntuoguole low uplift, Tarim Basin, western China. *AAPG Bull.* **2021**, *105* (1), 65−107.
(37) Bian, J. J.; Hou, D. J.; Cui, Y. W.; Zhu, X. X. Geochemical characteristics and origin of the ultra-deep hydrocarbons from the Shunbei Oilfield in the Tarim Basin, China: Insight from molecular biomarkers and carbon isotope geochemistry. *Mar. Pet. Geol.* **2023**, *158*, 106542.
(38) Qi, Y.; Sun, P.; Cai, C. F.; Wang, D. W.; Peng, Y. Y. Phase fractionation controlling regional distribution of diamondoids: A case study from the Halahatang oil field, Tarim Basin, China. *Mar. Pet. Geol.* **2022**, *140*, 105674.
(39) Chen, S.; Zhang, Y. T.; Xie, Z.; Song, X. G.; Liang, X. X. Multi-stages of Paleozoic deformation of the fault system in the Tazhong Uplift, Tarim Basin, NW China: Implications for hydrocarbon accumulation. *J. Asian Earth Sci.* **2024**, *265* (15), 106086.
(40) Xiao, X. M.; Song, Z. G.; Liu, D. H.; Liu, Z. F.; Fu, J. M. The Tazhong hybrid petroleum system, Tarim Basin, China. *Mar. Pet. Geol.* **2000**, *17* (1), 1−12.
(41) Li, Q.; Jiang, Z. X.; Hu, W. X.; You, X. L.; Hao, G. L.; Zhang, J. T.; Wang, X. L. Origin of dolomites in the Lower Cambrian Xiaoerbulak Formation in the Tarim Basin, NW China: Implications for porosity development. *J. Asian Earth Sci.* **2016**, *115*, 557−570.
(42) Jia, C. Z.; Wei, G. Q. Structural characteristics and petroliferous features of Tarim Basin. *Chin. Sci. Bull.* **2002**, *47*, 1−11.
(43) Ma, Y. S.; Cai, X. Y.; Yun, L.; Li, Z. J.; Li, H. L.; Deng, S.; Zhao, P. R. Practice and theoretical and technical progress in exploration and development of Shunbei ultra-deep carbonate oil and gas field, Tarim Basin, NW China. *Pet. Explor. Dev.* **2022**, *49* (1), 1−20.
(44) Chen, J. J.; He, D. F.; Tian, F. L.; Huang, C.; Ma, D. B.; Zhang, W. K. Control of mechanical stratigraphy on the stratified style of strike-slip faults in the central Tarim Craton, NW China. *Tectonophysics* **2022**, *830*, 229307.
(45) Wang, Q. R.; Huang, H. P.; Chen, H. H.; Zhao, Y. T. Secondary alteration of ancient Shuntuoguole oil reservoirs, Tarim Basin, NW China. *Mar. Pet. Geol.* **2020**, *111*, 202−218.
(46) Bray, E. E.; Evans, E. D. Distribution of n-paraffins as a clue to recognition of source beds. *Geochim. Cosmochim. Acta* **1961**, *22* (1), 2−15.
(47) Qiao, R. Z.; Li, M. J.; Zhang, D. L.; Xiao, H. Geochemistry and accumulation of the ultra-deep Ordovician oils in the Shunbei oilfield, Tarim Basin: Coupling of reservoir secondary processes and filling events. *Mar. Pet. Geol.* **2024**, *167*, 106959.
(48) Dai, J. X. Identification a distinction of various alkane gases. *Sci. China, Ser. B: Chem.* **1992**, *35*, 1246.
(49) Sun, Y. G.; Xu, S. P.; Lu, H.; Cuai, P. X. Source facies of the Paleozoic petroleum systems in the Tabei uplift, Tarim Basin, NW China: implications from aryl isoprenoids in crude oils. *Org. Geochem.* **2003**, *34* (4), 629−634.
(50) Cai, C. F.; Zhang, C. M.; Worden, R. H.; Wang, T. K.; Li, H. X.; Jiang, L.; Huang, S. Y.; Zhang, B. Application of sulfur and carbon isotopes to oil−source rock correlation: A case study from the Tazhong area, Tarim Basin, China. *Org. Geochem.* **2015**, *83*−*84*, 140−152.
(51) Thompson, K. F. M. Classification and thermal history of petroleum based on light hydrocarbons. *Geochim. Cosmochim. Acta* **1983**, *47* (2), 303−316.
(52) Walters, C. C.; Isaksen, G. H.; Peters, K. E. Applications of light hydrocarbon molecular and isotopic compositions in oil and gas exploration. In *Analytical Advances for Hydrocarbon Research*; Hsu, C. S., Ed.; *Modern Analytical Chemistry*; Springer: Boston, MA, 2003.
(53) Thompson, K. F. M. Fractionated aromatic petroleums and the generation of gascondensates. *Org. Geochem.* **1987**, *11* (6), 573−590.
(54) Moldowan, J. M.; Dahl, J.; Zinniker, D.; Barbanti, S. M. Underutilized advanced geochemical technologies for oil and gas exploration and production-1. The diamondoids. *J. Pet. Sci. Eng.* **2015**, *126*, 87−96.
(55) Qiao, R. Z.; Li, M. J.; Zhang, D. L.; Chen, Z. H.; Xiao, H. Evaporative Fractionation as the Important Formation Mechanism of Light Oil Reservoirs in the Dongying Depression, NE China. *Energies* **2024**, *17*, 3734.
(56) Luemba, M.; Chen, Z. H.; Ntibahanana, J. Molecular markers of Neoproterozoic-Lower Paleozoic petroleum systems and their geological significance: A case study of the cratonic basins in western China. *J. Pet. Sci. Eng.* **2021**, *204*, 108707.
(57) Xu, H. Y.; Liu, Q. Y.; Zhu, D. Y.; Meng, Q. Q.; Jin, Z. J.; Fu, Q.; George, S. C. Hydrothermal catalytic conversion and metastable equilibrium of organic compounds in the Jinding Zn/Pb ore deposit. *Geochim. Cosmochim. Acta* **2021**, *307*, 133−150.
(58) Song, D. F.; Zhang, C. M.; Li, S. M.; Wang, T. G.; Li, M. J. Elevated Mango's K1 Values Resulting from Thermochemical Sulfate Reduction within the Tazhong Oils, Tarim Basin. *Energy Fuels* **2017**, *31*, 1250−1258.
(59) Richard, L. Calculation of the standard molal thermodynamic properties as a function of temperature and pressure of some geochemically important organic sulfur compounds § §This paper is dedicated to Professor Harold C. Helgeson on the occasion of his seventieth birthday. *Geochim. Cosmochim. Acta* **2001**, *65* (21), 3827−3877.
(60) Yang, S. B.; Li, M. J.; Liu, X. Q.; Han, Q. Y.; Wu, J.; Zhong, N. N. Thermodynamic stability of methyldibenzothiophenes in sedimentary rock extracts: Based on molecular simulation and geochemical data. *Org. Geochem.* **2019**, *129*, 24−41.
(61) Wu, J.; Qi, W.; Luo, Q. Y.; Chen, Q.; Shi, S. B.; Li, M. J.; Zhong, N. N. Experiments on the generation of dimethyldibenzothiophene and its geochemical implications. *Pet. Geol. Exp.* **2019**, *41* (2), 260−267.

https://doi.org/10.1021/acs.energyfuels.4c02159
Energy Fuels 2024, 38, 18413−18430

(62) Li, D.; Chang, J.; Qiu, N. S.; Wang, J. S.; Zhang, M. R.; Wu, X.; Han, J.; Li, H. L.; Ma, A. L. The thermal history in sedimentary basins: A case study of the central Tarim Basin, Western China. *J. Asian Earth Sci.* **2022**, *229*, 105149.
(63) White, C. M.; Lee, M. L. Identification and geochemical significance of some aromatic components of coal. *Geochim. Cosmochim. Acta* **1980**, *44* (11), 1825−1832.
(64) van Aarssen, B. G. K.; Bastow, T. P.; Alexander, R.; Kagi, R. I. Distributions of methylated naphthalenes in crude oils: indicators of maturity, biodegradation and mixing. *Org. Geochem.* **1999**, *30* (10), 1213−1227.
(65) Armstroff, A.; Wilkes, H.; Schwarzbauer, J.; Littke, R.; Horsfield, B. The potential role of redox reactions for the distribution of alkyl naphthalenes and their oxygenated analogues in terrestrial organic matter of Late Palaeozoic age. *Org. Geochem.* **2007**, *38* (10), 1692−1714.
(66) Xiao, F.; Liu, L. F.; Zhang, Z. H.; Wu, K. J.; Xu, Z. J.; Zhou, C. X. Conflicting sterane and aromatic maturity parameters in Neogene light oils, eastern Chepaizi High, Junggar Basin, NW China. *Org. Geochem.* **2014**, *76*, 48−61.
(67) Zhang, M. M.; Li, Z. Thermal maturity of the Permian Lucaogou Formation organic-rich shale at the northern foot of Bogda Mountains, Junggar Basin (NW China): Effective assessments from organic geochemistry. *Fuel* **2018**, *211* (4), 278−290.
(68) Huang, W. Y.; Zhang, H. Z.; Xiao, Z. Y.; Yu, S.; Pan, C. C. Generation, expulsion, and accumulation of diamondoids, aromatic components and gaseous hydrocarbons for gas fields in Kuqa Depression of the Tarim Basin, NW China. *Mar. Pet. Geol.* **2022**, *145*, 105893.
(69) Bastow, T. P.; Alexander, R.; Sosrowidjojo, I. B.; Kagi, R. I. Pentamethylnaphthalenes and related compounds in sedimentary organic matter. *Org. Geochem.* **1998**, *28* (9−10), 585−595.
(70) Wei, Z.; Moldowan, J. M.; Fago, F.; Dahl, J. E.; Cai, C.; Peters, K. E. Origins of thiadiamondoids and diamondoidthiols in petroleum. *Energy Fuels* **2007**, *21*, 3431−3436.
(71) Fang, C. C.; Xiong, Y. Q.; Li, Y.; Chen, Y.; Liu, J. Z.; Zhang, H. Z.; Adedosu, T. A.; Peng, P. A. The origin and evolution of adamantanes and diamantanes in petroleum. *Geochim. Cosmochim. Acta* **2013**, *120*, 109−120.
(72) Qiao, R. Z.; Chen, Z. H.; Li, C. Y.; Wang, D. Y.; Gao, Y.; Zhao, L. Q.; Li, Y. Q.; Liu, J. Y. Geochemistry and accumulation of petroleum in deep lacustrine reservoirs: A case study of Dongying Depression, Bohai Bay Basin. *J. Pet. Sci. Eng.* **2022**, *213*, 110433.
(73) Wu, P.; Hou, D. J.; Gan, J.; Li, X.; Ding, W. J.; Liang, G.; Wu, B. B. Paleoenvironment and Controlling Factors of Oligocene Source Rock in the Eastern Deep-Water Area of the Qiongdongnan Basin: Evidences from Organic Geochemistry and Palynology. *Energy Fuels* **2018**, *32* (7), 7423−7437.
(74) Chen, K. F.; Zhang, C.; Zhou, S. X.; Li, J.; Liu, S. L. Light Hydrocarbon (C_5−C_7) Geochemistry in the Northern Margin of the Qaidam Basin, Northeastern Tibetan Plateau: Gas Mixing and Hydrocarbon Charge History. *ACS Omega* **2021**, *6* (48), 32709−32721.

https://doi.org/10.1021/acs.energyfuels.4c02159
Energy Fuels 2024, 38, 18413−18430